Groundwater for Sustainable Development 11 (2020) 100463

Contents lists available at ScienceDirect

Groundwater for Sustainable Development

journal homepage: http://www.elsevier.com/locate/gsd

Review article

The use of micro-nano bubbles in groundwater remediation: A comprehensive review

Sabeera Haris [a], Xiaobin Qiu [a], Harald Klammler [b,c], Mohamed M.A. Mohamed [a,d,*]

[a] Civil and Environmental Engineering Department, College of Engineering, United Arab Emirates University, Al Ain, 15551, United Arab Emirates
[b] Department of Geosciences, Federal University of Bahia, Salvador, Bahia, Brazil
[c] Engineering School for Sustainable Infrastructure and Environment (ESSIE), University of Florida, Gainesville, USA
[d] National Water Center, United Arab Emirates University, Al Ain, 15551, United Arab Emirates

ARTICLE INFO

Keywords:
Micro-nano bubbles
Generation
Properties
Groundwater remediation
Review

ABSTRACT

Micro-nano bubbles (MNBs) are minute bubbles with diameters on the micrometer and nanometer scale. Along with small size, MNBs have a large specific surface area, high zeta potential, long residence times in water, and high oxygen transfer efficiency. These attributes make MNBs more effective than conventional macro-bubbles in air sparging for groundwater remediation purposes. This paper aims to review recent research on the generation and properties of MNBs, and its implementation as a groundwater remediation technology. The MNB generation techniques are categorized while the factors to choose bubble generators are analyzed. Methods for characterization of MNB properties, including size and zeta potential, are also summarized. We further discuss properties and controlling factors of MNBs' size, mass transfer, rising velocity, zeta potential, transport and generation of hydroxyl radicals in water. We summarize recent findings related to the use of MNBs technologies for remediation of contaminated groundwater bodies. Finally, the current challenges and limitations of MNBs application for groundwater remediation are discussed.

1. Introduction

Air sparging is a groundwater remediation technique where a gas, usually air, is pumped into an area beneath the water table through a network of injection wells. The injected air forces deep groundwater to circulate and aerates the water to removes volatiles. Furthermore, the air sparging process enhances groundwater remediation as it provides increased amounts of oxygen for biodegradation (Interstate Technology and Regulatory Council, 2005). That relies on the process of mass transfer between the gas and liquid phase, in combination with the phenomena of diffusion and mixing in the water (Droste, 1996; Elserwy, 2019). In general, air sparging targets sites where groundwater and/or saturated soils are contaminated with volatile, semi-volatile, and/or non-volatile aerobically biodegradable organic contaminants (Miller, 1996). Conventionally air bubbles with diameters in the range of 2–5 mm (macrobubbles) are employed. However, recent studies of water treatment with MNBs in the lab have shown that MNBs can increase the efficiency of mass transfer and produce higher dissolved oxygen concentrations (Chen et al., 2008; Eamrat et al., 2020; Jiang and Wu, 2011; Suwartha et al., 2020). Advanced oxidation and ozonation technology is gaining more attention in water pollution control, particularly, the MNBs technology. It has broad applications and prospects for water treatment in terms of enhancing gas-liquid mass transfer, improving the utilization of oxidizing free radicals and oxidizing capacity due to its characteristics (Fan et al., 2020; Li et al., 2014; Ma et al., 2015; Shi et al., 2018; Xiao et al., 2018; Yujing, 2018; Zhang et al., 2020a).

Most of the available review papers focus on a single kind of bubbles and very specific aspects, such as mass transport, stability theories, ozonation, etc. (Table 1). Much effort has been made on collecting and summarizing MNBs' generation methods, properties, or applications (using ozone, air or oxygen) in water and wastewater treatment (Agarwal et al., 2011; Alheshibri et al., 2016; Azevedo et al., 2019; Khuntia et al., 2012; Parmar and Majumder, 2013; Shangguan et al., 2018; Sun et al., 2016; Tekile et al., 2017; Temesgen et al., 2017). There is limited content on the upscaling of MNB applications to the industrial level, mathematical modeling of contaminant removal, and up-to-date analyses of the current challenges and future perspectives. In this paper, we provide a comprehensive review of fundamental topics including

* Corresponding author. Civil and Environmental Engineering Department, College of Engineering, United Arab Emirates University, Al Ain, 15551, United Arab Emirates.
E-mail address: m.mohamed@uaeu.ac.ae (M.A. Mohamed).

https://doi.org/10.1016/j.gsd.2020.100463
Received 2 March 2020; Received in revised form 20 July 2020; Accepted 28 July 2020
Available online 1 August 2020

Table 1
Content summaries of previous reviews.

Num	Title	Author and Year	Content
1	Principle and applications of microbubble and nanobubble technology for water treatment	Agarwal et al. (2011)	Generation of free radicals by microbubbles; physics, generation, bubble size of MNBs; MNBs in water treatment (degradation of organic pollutants, disinfection, cleaning and defouling of solid surfaces).
2	Microbubble-aided water and wastewater purification: A review	Khuntia et al. (2012)	Structure, properties, generation, gas transportation of microbubbles; applications of microbubbles with ozone; air and oxygen microbubbles in water and wastewater treatment.
3	Microbubble generation and microbubble-aided transport process intensification—A state-of-the-art report	Parmar and Majumder (2013)	Microbubble-aided transport process; components, properties, generation, characterization of Microbubbles.
4	Stability theories of nanobubbles at solid–liquid interface: A review	Sun et al. (2016)	Research progresses and suggestions of stability theories of nanobubbles.
5	A History of Nanobubbles	Alheshibri et al. (2016)	Timeline of significant finding of surface and bulk nanobubbles: theory of bubble growth and dissolution; evidence, characterization, production, uses and potential applications of nanobubbles.
6	Micro and nanobubble technologies as a new horizon for water-treatment techniques: A review	Temesgen et al. (2017)	Definition, classification, generation, properties of MNBs; applications of MNBs in the water treatment processes (aeration, flotation, and disinfection).
7	Applications of Ozone Micro- and Nanobubble Technologies in Water and Wastewater Treatment: Review	Tekile et al. (2017)	Ozone MNBs in disinfection, oxidation of organic and inorganic pollutants, color removal of water and wastewater treatment; the future of ozone MNBs.
8	A Review of Microbubble and its Applications in Ozonation	Shangguan et al. (2018)	Properties and generation of microbubbles; applications in ozone treatment.
9	Bulk nanobubbles in the mineral and environmental areas: Updating research and applications	Azevedo et al. (2019)	A brief summary of nanobubbles' application in different field; generation, stability and characterization of nanobubbles; specific applications of nanobubbles in environmental and mineral processing area.

updates of the most recent research outcomes and guidelines for MNB characterization that are expected to be particularly helpful at the introductory level, i.e., to researchers from related fields who started to gain interest in this fast-growing field.

2. What are the MNBs

2.1. Definition of MNBs

MNBs are minute gas bubbles with diameters on the order of micrometers and nanometers (Alheshibri et al., 2016; Li et al., 2013a). Microbubbles (MBs) and nanobubbles (NBs) are tiny bubbles with a respective diameter of >1 μm and <1 μm approximately. Different researches will have different size ranges (Agarwal et al., 2011; Alheshibri et al., 2016; Atkinson et al., 2019; Fan et al., 2020; Hu and Xia, 2018). Before 21st century, due to the thermodynamic stability problem, the existence of NBs was not widely accepted and caused a long-term debate. But in the recent years, with the merging of new technologies, such as dynamic light scattering, acoustic spectroscopy, electron microscopy, etc., more and more evidence accumulates to prove the existence and possible stability of NBs (Alheshibri and Craig, 2019; Jadhav and Barigou, 2020; Ushikubo et al., 2010b; Yasui et al., 2018). Overall, there are two kinds of NBs: surface NBs at aqueous surface and bulk NBs in aqueous solution (Alheshibri et al., 2016). The application of MNBs in environmental remediation and bioremediation has garnered recent attention owing to their special characteristics, including large specific surface area, negatively charged surface, long residence time in water, high mass transfer efficiency, and the generation of highly reactive free radicals (Koshoridze and Levin, 2019; Li et al., 2014; Qian et al., 2019; Rosa and Rubio, 2018; Wang et al., 2018). These studies showed that MNBs greatly augment remediation by accelerating the oxygen transfer process (Li et al., 2013b).

2.2. Comparison with macrobubbles

A critical factor in enhancing the efficiency of remediation of contaminated water is the transfer of a treatment substance (e.g., oxygen) into the water (mass transfer coefficient). The aerobic biodegradation capacity is related to the growth of site specific microorganisms, which is significantly affected by the oxygen content in water (Song and Katayama, 2010; Tanaka et al., 2020). Conventional air sparging techniques employ macrobubbles with diameters of millimeters or centimeters, which have short residence times in groundwater and are inefficient for the oxygen transfer process, leading to a small zone of influence (ZOI) around bubbles and low activity of aerobic microorganism. Mass transfer coefficients for macrobubbles were found to be approximately constant, whereas for MNBs (less than 40 μm) they increase with decreasing diameter (Hu et al., 2010; Skouteris et al., 2020), thus making them a more effective technique (Li et al., 2014; Liu and Tang, 2019). MBs with a 30-μm radius were first identified in water by Turner (1961) and they were found to exist for long periods of time. Similarly, NBs also exist in water for longer periods and this stability can be attributed to an electrically charged liquid-gas interface, creating repulsion forces that prevent bubble coalescence. NNB surfaces are negatively charged with an electric double layer and the external electrostatic pressure balances the internal Laplace pressure. (Nirmalkar et al., 2018a, 2018b; Ushikubo et al., 2010b).

2.3. The structure of MNBs

MBs are enclosed by two concentric gas spheres (Fig. 1), which are separated by a layer of water in between (Guo et al., 2019; Khuntia et al., 2012). The gas phase may comprise a single gas or a combination of gases; gas combinations generally create differentials in partial pressure and gas osmotic pressures, which stabilize the bubbles. The gas phase is enclosed by a liquid shell. Diffusion of gas out of MBs and the mechanical properties of MBs depend on the shell material. The liquid phase is the external liquid surrounding the shell in which the bubble resides; it can be the same as the shell material, or it can be a surfactant or foaming agent depending upon the operations (Parmar and Majumder, 2013). For NBs (Fig. 2), the system of gas and liquid can be

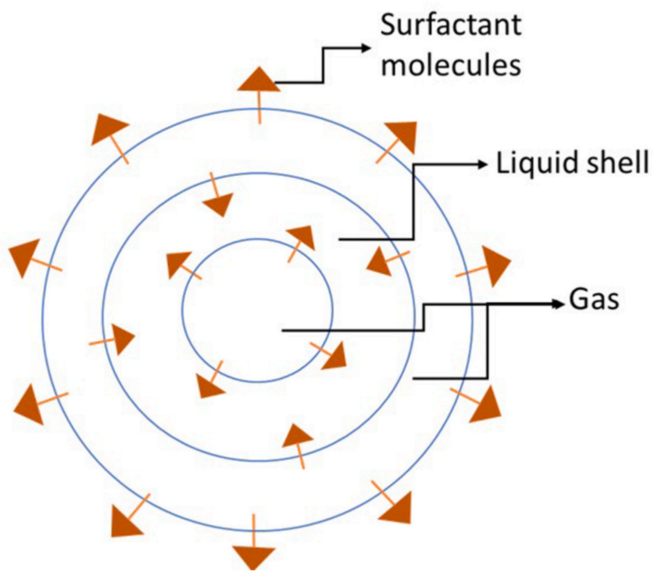

Fig. 1. The concentric gas-sphere model of a surfactant-stabilized MB(Khuntia et al., 2012).

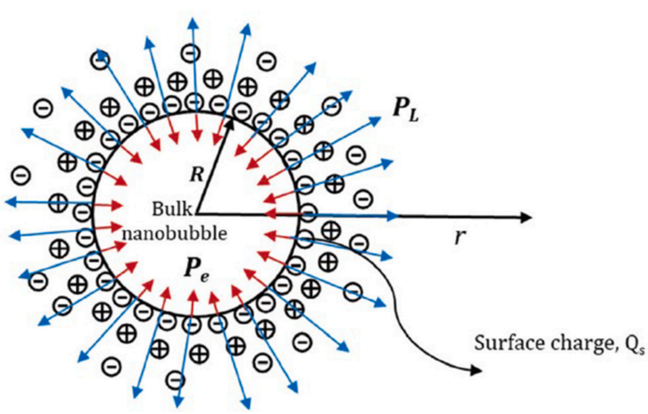

Fig. 2. Schematic representation of the Laplace and electrostatic pressures acting on a bulk NB (radius of NB R, surface charge Q_s, the electrostatic pressure P_e, Laplace pressure P_L, radius of the charge distribution r) (Nirmalkar et al., 2018b).

assumed to be in thermodynamic equilibrium at a certain fixed temperature and pressure. The presence of ions in the bulk liquid constitutes an electric double layer and the adsorbed ions at the interface are expected to exert an external inward radial force due to Coulomb interactions (Nirmalkar et al., 2018b).

3. Methods for characterization of MNBs

3.1. Size measurement

For particle size, there are many commercially available techniques: dynamic light scattering (same as photon correlation spectroscopy), static light scattering, electron microscopy (scanning electron microscope), atomic force microscopy, laser scanners, acoustic spectroscopy, optical microscopy (Geisse, 2009; Hain et al., 2019), image analysis, etc. Among them, the most common ones are dynamic light scattering, atomic force microscopy and image analysis (Table 2).

Although atomic force microscopy and electron microscopy can provide the information about the material in nanometer scale, electron microscopy is good at determining the composition of a material. But for the operating environment, atomic force microscopy can be used in a vacuum, ambient, gas or liquid environment, whereas the electron microscopy is only suitable in a vacuum environment (Smith, 2015). So the atomic force microscopy is more widely used for MNBs, focusing on the NB characterization NB surface properties, such as the shell thickness (Huang et al., 2020c; Shafi et al., 2019).

Even though the image analysis is widely employed to characterize MNB size, it has some restrictions in usage, such as a transparent barrier required to take an image, high resolution and speed of cameras, and a low concentration of bubble (Juwana et al., 2019; Li et al., 2019a; Swart et al., 2020; Zhang et al., 2020b). In some studies, the image analysis is combined with other techniques to increase the effectiveness of measurement (Bae et al., 2020; Juwana et al., 2018). In more recent applications, optical microscopy resolution is on the order of 200–500 nm which allows measurements on MBs, but not NBs (Geisse, 2009; Huszka and Gijs, 2019).

Static and dynamic light scattering techniques study the structure and dynamics of scattering objects in solution. Static light scattering measures the angular distribution of the scattering intensity to infer structural information from objects. In contrast, dynamic light scattering is the extension of elastic light scattering to study inhomogeneous dynamic systems by measuring the fluctuations in scattered light intensities caused by Brownian motion (Ahrer et al., 2003; Klemeshev et al., 2016; Park et al., 2010). Therefore, dynamic light scattering is more common for MNB applications. However, this technique is an ensemble-average approach which only provides the average particle size and associated distribution. In addition, it requires strong light scattering to calculate the scattered light intensities and does not inform bubble concentration. The accuracy is only high for solid particles measurement, not for MNBs. To tackle these problems, nanoparticle tracking analysis is utilized to analyze particle size and count (Midtvedt et al., 2020). Nanoparticle Tracking Analysis separately tracks the movement trajectory of each particle in the field of view to obtain the particle size information of each particle. It has obvious advantage for small particles and weakly scattered sample particles, especially for bulk NBs (Griffiths et al., 2020; Hu and Xia, 2018; Thonglek et al., 2019).

3.2. Zeta potential measurement

The zeta potential is the electro-kinetic potential in colloidal systems, and it is an important bubble surface characteristic related to the stability of MNBs. From a theoretical viewpoint, zeta potential is the electric potential in the interfacial double layer of a dispersed particle or droplet versus a point in the continuous phase away from the interface (Clogston and Patri, 2011; Wei Lu and Ping, 2010). Lower absolute zeta potential values will lead to aggregation, coagulation, or flocculation due to van der Waals interparticle attraction (Jabra Shnoudeh et al., 2019).

There are three methods for zeta potential determination of suspended particles: single particle observation, acoustical methods, and electrophoretic light scattering. Single particle observation has the problem of interfering electro-osmotic velocity due to the cell walls and a lower limit of particle size. Acoustical methods depend on the complex and not yet fully understood relations among acoustic and electro-acoustic properties, particle size distribution, charge density and concentration. Because of their sensitivity, accuracy, and versatility, electrophoretic light scattering is the best choice (Weiner and Zhang, 2013; Xu, 2008). Electrophoretic light scattering applies an external electric field to the sample, the charged particles in solution will move accordingly. The velocity of the particles is measured by the interference of the scattered light with the help of laser Doppler velocimetry. Using some appropriate theoretical models (such as the Henry function), the zeta potential is determined from the electrophoretic mobility, which can be calculated by the measured velocity and the amplitude of the electric field (Clogston and Patri, 2011; Huang et al., 2020a).

Table 2
Methods for MNB size measurement.

Num	Title	Author and Year	Bubble size	Equipment	Method
1	Hydrodynamic characteristics of the microbubble dissolution in liquid using orifice type microbubble generator	Juwana et al. (2019)	0 μm −2400 μm	High-speed camera using shadow photographic tech-nique	Image analysis
2	Characterization of micro-bubble size distribution and flow configuration in DAF contact zone by a non-intrusive image analysis system and tracer tests	Moruzzi and Reali (2010)	10 μm −100 μm	Nikon 5400 digital camera attached to magnifying lens	Image analysis
3	Correspondence of gas holdup and bubble size in presence of different frothers	Azgomi et al. (2007)	300 μm −1000 μm	McGill bubble size analyzer	Image analysis
4	Investigation of condition-induced bubble size and distribution in electroflotation using a high-speed camera	Ren et al. (2014)	20 μm–1000μm	High-speed camera with using Image-Pro® Plus and SigmaScan® Pro software	Image analysis
5	Bubble size distribution in a laboratory-scale electroflotation study	Alam et al. (2017)	32.7 μm–68.6 μm	High-speed camera.	Image analysis
6	Statistical analysis of jet drop generation based on bubble size measurements in the pickling process	Wang et al. (2019)	70 μm −1800 μm	High-speed camera capturing 960 × 720 pixel images	Image analysis
7	Preparation and characterization of perfluorocarbon microbubbles using Shirasu Porous Glass (SPG) membranes	Melich et al. (2019)	6 μm −60 μm	Laser diffraction particle size analysis (Mastersizer 3000, Malvern Instrumentation, France)	Image analysis
8	Morphological and force spectroscopy characterizations for indentification of surface nanobubbles from nanodroplets and blisters	Li et al. (2020)	0 nm–600 nm	Commercial atomic force microscope (Resolve, Bruker, U.S.A.)	Atomic force microscopy
9	Characterization of Bulk Nanobubbles Formed by Using a Porous Alumina Film with Ordered Nanopores	Ma et al. (2020)	0 nm–500 nm	Nanosight LM10 instrument (Malvern); atomic force microscope	Nanoparticle tracking analysis; atomic force microscopy
10	Effect of Micro- and Nanobubbles on the Crystallization of THF Hydrate Based on the Observation by Atomic Force Microscopy	Huang et al. (2020c)	200 nm–500 nm	Atomic force microscope (Dimension FastScan, Bruker Corporation)	Atomic force microscopy
11	Probing phospholipid microbubbles by atomic force microscopy to quantify bubble mechanics and nanostructural shell properties	Shafi et al. (2019)	0 nm–36 nm	Atomic force microscope (MFP-1D, Asylum Research, Santa Barbara, CA, USA)	Atomic force microscopy
12	Lability-specific enrichment of typical engineered metal (oxide) nanoparticles by surface-functionalized microbubbles from waters	Zhang et al., 2020c	48 nm-128nm	Mastersizer 3000 (Malvern Instruments Ltd., U.K.).	Dynamic light scattering
13	A novel flotation technique combining carrier flotation and cavitation bubbles to enhance separation efficiency of ultra-fine particles	Zhou et al. (2020)	20 nm-1200nm	Zeta Plus (Brookhaven, US)	Dynamic light scattering
14	Size and Refractive Index Determination of Subwavelength Particles and Air Bubbles by Holographic Nanoparticle Tracking Analysis	Midtvedt et al. (2020)	60 nm–400 nm	Nanosight LM10 instrument (Malvern)	Nanoparticle tracking analysis
15	Nanoparticle Tracking Analysis for Multiparameter Characterization and Counting of Nanoparticle Suspensions	Griffiths et al. (2020)	10 nm–1000 nm	Nanosight LM10 instrument (Malvern)	Nanoparticle tracking analysis
16	Identification of High Concentration Ultra-fine Bubbles in the Water	Thonglek et al. (2019)	0 nm–647 nm	Nanosight LM10 instrument (Malvern)	Nanoparticle tracking analysis
17	Application of ozone micro-nano-bubbles to groundwater remediation	Hu and Xia (2018)	32–460 nm	Nanosight LM10 instrument (Malvern)	Nanoparticle tracking analysis

3.3. *Other measurements*

Except size and zeta potential, there are many other properties of MNBs that may be of interest, and which may be investigated by modifications and/or combinations of different methods. Li et al. (2019a,b) used a high-speed camera at 125 fps equipped with a high magnification lens for bubble counting, while Bae et al. (2020) employed a Sony B01EINFC5W model and a magnification lens (Sony FE 28–70 mm) to observe bubble rising velocity. In addition, custom-designed image analysis software can be used to quantify MB oscillation (Beekers et al., 2020). The coalescence and movement of NBs on a graphene surface in water were investigated in detail by using the molecular dynamics simulation method (Li et al., 2018). When cavitation occurs in bubble generation, a characteristic high-frequency noise is emitted, such that cavitation inception could be measured using a microphone (Li et al., 2019a). A tensiometer and a Raman Spectrometer can be employed individually to find out surface tension and functional groups respectively (Zhang et al., 2019). Gas holdup fraction of micro-bubbles is studied using dynamic gas disengagement analysis and image analysis (Bae et al., 2020). Combined atomic force microscopy (AFM) and fluorescence lifetime imaging microscopy (FLIM) were conducted to localize the various interfaces and identify gas-filled (surface) NBs rapidly (Hain et al., 2019). A recent method known as nanoparticle tracking analysis (NTA) employs infrared absorption spectroscopy in the multiple internal reflection geometry and AFM to confirm the formation of NBs (Ma et al., 2020).

4. MNBs generation

4.1. *Selection of MNB generator*

When choosing a MNBs generator, a number of factors have to be considered carefully. First, it is the working environment where the generator is used, that is, in a laboratory or outside (e.g., in situ field application or in treatment plant). If outside, light-weight portable generators are of interest, while assuring that the capacity of bubbles production meets the projected needs for the expected volume of water to be treated. When dealing with water containing pollutants (sand, screenings, mud, erosive chemical, etc.), there are more challenges to overcome, involving problems, such as clogging, cleaning and/or erosion.

The second factor is the application/research purpose and requirement. Diverse MNBs generators generate bubbles of various size and concentration ranges. Some studies focus on the characterization of a single bubble; therefore, they need to produce bubbles in a very low concentration and facilitate isolation of individual bubbles. When investigating the features of bubbles with different sizes, a key issue is the capability of being able to easily change the bubble size through the generator set-up. If the work requires high clean conditions, the major consideration is on the prevention and removal of pollution from the bubble generator.

Last but not least, there is cost. For batch experiment, in most cases, the set-up of bubble generators is self-made or assembled by the researchers. The core parts would be purchased according to the principle of bubble generation. In the market, it is difficult to find a standardized generator for a specific application, since most of the work is still at the research level and, hence, novel in the sense that they are meant to fill a knowledge gap. In general, bubble generators are currently expensive and hard to modify. If the generator choice is related to MNBs application at a large scale, the costs of electricity and maintenance should be considered.

4.2. MNB generation techniques

Extensive research has been carried out on the ways in which MBs can be generated, which is documented by a comprehensive review (Parmar and Majumder, 2013). Although this paper reviewed the techniques or generators of MBs, most of the techniques or generators, if different working parameters are set, can produce the NBs as well nowadays. In their review, the bubble generators are categorized by the characteristics of the applied technique, which we summarize in Table 3 here for convenience. However, in what follows, we also provide a simpler classification depending on the main working principles of the techniques, which can be hydrodynamic, acoustic (sonication), electrochemical or mechanical agitation (Huang et al., 2020b).

4.2.1. Hydrodynamic method

The hydrodynamic method is based on the principle of cavitation, which causes the formation of small vapor-filled cavities (i.e., bubbles), where pressure in the liquid is sufficiently low (Agarwal et al., 2011). An orifice plate or a venturi tube are the most common tools to create hydrodynamic cavitation. The orifice type MB generator (the multi fluid mixture device) has an orifice in a flowing water tube, in which the water is pressurized to introduce into the generator. The difference in water velocity between the orifice and generator exit leads to the negative pressure at a small distance downstream of the orifice. That negative pressure sucks the air through a stainless steel perforated pipe embedded in the flowing water tube, which breaks the air into many MB by strong shear action (Sadatomi et al., 2012). Benny et al. replaced the perforated steel pipe with a porous ceramic pipe, which was made of a custom-made plastic scaffold and nylon fibers rolled around the scaffold. It enhanced the durability while also decreasing the production cost. In addition, it overcome the problems of other microbubble generators, such as the difficulties to mix the spherical body in smaller generator and drill small holes (Pambudiarto et al., 2020; Sadatomi et al., 2005).

The venturi type of generator has three main components, being a converging part, a throat, and a diverging part. Simple structure, high reliability, excellent efficiency, and a wide range of potential applications are the benefits of venturi type generators (Huang et al., 2020b; Stride and Edirisinghe, 2009). The venturi tube geometry has dominant impact on the local pressure and cavitation, thereby controlling the bubble size and energy efficiency. From the results of simulation and experiment, the throat pressure and power consumption are significantly influenced by the outlet angle and the diameter ratio (Li et al., 2019a). Venturi-porous pipe MB generator combined venturi tube and porous pipe, such that it may also be seen as a modification of the orifice type. Recent literature reviews considered ease of the manufacturing process and recommended certain inlet angle (20°) and outlet angle (12°) for the venturi-porous pipe MB generator (Huang et al., 2020b; Majid et al., 2018).

Table 3
Categories and types of microbubble generation (Parmar and Majumder, 2013).

Num	Category	Types
1	When flowing liquid is used	Spherical body in a flowing tube, Rotary liquid flow type, Static mixture type, Venturi type, Ejector type, Multi fluid mixture device, Pressurized dissolution type
2	Without accompanying liquid flow	Rotary gas flow type, Porous membrane type, Electrolysis type, Vapor condensation system, Porous mullet ceramics technique
3	By polymer	Emulsion solvent vaporization, Cross linking polymerization, Atomization and reconstitution
4	Low power generation techniques	Flow focusing technique, Microchannel technique, Ultrasonic systems, Micro-bubbler technique, Heating of carbon nanotube, Laser-induction breakdown in water, Using organic membrane, Shear flow in pipe and slits, Generation of single microbubble, Fiber optic tips coated with nano particles
5	Other methods	Electrostatic spraying, Microbubble generation by rotational porous plate, Co-axial electrohydrodynamic atomization, Spinning disk type microbubble generator

4.2.2. Acoustic method

Most of the generators using the hydrodynamic method, such as static mixer, swirl liquid flow method, etc., involve a liquid pump for gas-liquid two-phase fluid. Such generators would require circulation between the generator and the water tank for many times, therefore, a longer operation time is needed to generate the MNBs. Due to complicated components, hydrodynamic generators are relatively large. Acoustic bubble generators can overcome some drawbacks related to hydrodynamic methods (Morito and Makuta, 2018; Numakura et al., 2014; Yasuda et al., 2019). They are compact and simple in operation. Furthermore, the acoustic techniques can make bubble generation free of contamination, since the set-up does not need a liquid pump. Compared with mechanical agitation (see section 4.2.3 below), the sonication presents better performance in surfactant systems, having higher gas hold-up, smaller bubble size, and larger interfacial area (Xu et al., 2008). NBs of mode diameter between 90 and 100 nm were made by the ultrasonic irradiation experiments to water (Yasuda et al., 2019). The results demonstrated that the ultrasonic irradiation not only generated NBs but also reduced NBs, thereby approaching a certain bubble concentration. In two kinds of water (ultrapure water without NBs and water with a high NB concentration), the concentration of NBs exponentially changed with time and converged to an equilibrium value (Yasuda et al., 2019). The acoustic technique has great potential to control bubble size and bubble concentration with high accuracy. However, acoustic systems are more complicated than other techniques, even if it is highly automatic and compact.

4.2.3. Mechanical agitation method

Mechanical agitation typically consists in stirring the liquid and bubble generation depends on the mixer's or homogenizer's speed. It is less complex than other technologies, but the bubble sizes are relatively large and inhomogeneous. The acoustic method can create more homogenous and smaller MBs, while the hydrodynamic method performs best for the generation of a large number of MBs at once (Yamaguchi et al., 2018). Consequently, due to larger sizes and lower concentrations (smaller gas hold-up) of bubbles, generators using mechanical agitation are less efficient in terms of solvent extraction and mass transfer. Therefore, it has increasingly lost its role as traditional method for bubble generation in the past (Daryabor et al., 2017; Shams et al., 2016; Xu et al., 2008; Zimmerman et al., 2007).

4.2.4. Electrochemical method

The electrochemical method is based on electrolysis, where MNBs are generated on electrodes submerged in a surfactant solution. During water electrolysis, the flow of electric current through the water between the electrodes triggers redox reactions generating oxygen and hydrogen at the cathode and anode, respectively. Surfactant is added into the solution to enhance MNB stability otherwise on a timescale 1 ms (HONG et al., 2020; Lucero et al., 2017; Maxwell, 2020; Svetovoy et al., 2020). On a short-time scale of ~10 μs, accompanying with a high relative super-saturation, high current causes homogenous nucleation of NBs. These NBs aggregate to MBs with time, which may be intensified by higher temperatures (Svetovoy et al., 2013). The NaCl concentration, pH and electrode distance showed obvious influence on the MNBs generation by electrolysis, while current density also exerted a great impact and was positively related to the bubble generation rate. Higher NaCl content and shorter distance between electrodes significantly reduced the power requirement. Compared with other types of anodes (iron, stainless steel, dimensionally sable anode), aluminum anode is more efficient (Lucero et al., 2017). Results in-situ study using a special designed single-channel electrolyzer indicated that all the bubbles were produced at the interface between the proton exchange membrane and the electrode wire (Li et al., 2019b). An increasing flow velocity reduced the detachment diameter whereas a higher current density lead to stronger bubble coalescence (Li et al., 2019b).

Alternating polarity (AP) voltage pulses in water electrolysis generates a high concentration of bulk NBs (~150 nm) filled with H_2 and O_2. For larger AP pulse magnitudes, MB (40 μm) are generated. The size grows to 300 μm and disappears completely in very short time. This phenomenon can be explained by the spontaneous combustion of H_2 and O_2 (Postnikov et al., 2018, 2016; Svetovoy et al., 2020, 2013, 2011). Tunable MB generators using electrolysis and ultrasound can produce stable mono-dispersed MBs in pure water. In this technology, the inertial constraints of microfluidics are overcome and additional surfactants are avoided. Experimental results show that a feed-back loop enables the generator to manipulate the bubble diameter easily over a wide range (Achaoui et al., 2017). However, the MNB collapse harmfully affects and erodes the surfaces of the electrodes causing pollutant from the electrodes into the solution. Moreover, owing to the water electrolysis, the generated MNB are filled with oxygen and hydrogen. Thus, the explosion of hydrogen is a major threat to the operator and safety is a key issue, if these gases accumulate in the working environment.

4.2.5. Other emerging methods

Recent developments in bubble generation is based on the combination or modification of different existing techniques. They have the advantages of simple construction, easy maintenance, less energy consumption and smaller manufacture cost. Such methods include repeated compression of MBs (Jin et al., 2019), layer-by-layer assembled SLIPS (Aghdam et al., 2019), nanosecond laser pulses (Fales et al., 2019), sonic-electrochemical method (Komaba and Goto, 2019).

5. Properties of MNBs and their controlling factors

5.1. Bubble size

The most studied property of air bubbles is bubble size. Based on the differences in their sizes, bubbles are categorized as macrobubbles, MBs, and sub-micron bubbles or NBs corresponding to conventional or big bubbles, fine bubbles, and ultrafine bubbles, respectively. Bubble size ranges and their associated properties are summarized in Table 4 (Agarwal et al., 2011; Pérez-Garibay et al., 2012; Tanaka et al., 2020; Temesgen et al., 2017; Xiao and Xu, 2020). Bubble size is the most basic property of the MNBs because other properties derive from it. A certain relationship was observed between the zeta potential of the NBs and their size (Zhang et al., 2020b). Macrobubbles are strongly affected by buoyancy and rising velocity with a consequent lack of stability during measurements. However, for MNBs the longer residence time in the liquid makes measurements more feasible (Ushikubo et al., 2010a). Bubble size is generally dynamic, that is, NBs can form after MBs shrinkage, while NBs can coalesce to become MBs (Jin et al., 2020; Sangbeom Kim et al., 2018).

Table 4
Bubble size ranges and major properties.

Bubble type	Diameter range (μm)	Properties
Macro-bubble/ traditional bubble	10^2–10^4	• Bursts at the surface • Rises fast (retention time: seconds) • Poor mass transfer • Small surface area to volume ratio • Less hydroxyl radical • Low gas pressure
Microbubble	1–10^2	• Bursts in the bulk liquid • Rises slowly (retention time: minutes) • Good mass transfer • Large surface area to volume ratio • More hydroxyl radical • Medium gas pressure
Nano/ultrafine bubble	10^{-3}–1	• Shrinks and bursts in the bulk liquid • Brownian motion (retention time: hours–months) • Higher mass transfer • Hugh surface area to volume ratio • More hydroxyl radical • High gas pressure

There are many factors impacting bubble size including pressure, fluid flow rate, air flow rate, the surface-active agents (surfactants, frothers, etc.) or electrolytes. The size distributions of MBs and NBs are also affected by the design and operational conditions, such as the pressure differences across the nozzle system of a generator (Kim et al., 2012). Higher pressure produces smaller bubbles because of an increase in air density, and at pressures above approximately 3.5 atm, the sizes of MBs are almost constant. The MNB size is also affected by the injection rates of water and gas (Hu and Xia, 2018). Moreover, bubble size decreases when surfactant concentration or liquid flow rate are raised, while it increases with increasing air pressure and flow rate. The higher air pressure leads to larger inlet pressure at a cavitation tube, therefore, contributes to a larger energy dissipation and stronger turbulence. It intensifies cavity collapse and results in bigger bubbles (Juwana et al., 2018; Majid et al., 2018; Zhang et al., 2020a). The addition of frothers (chemical additives used in the flotation processes to facilitate generation of fine bubbles and reduce bubble coalescence) and electrolyte solutions containing NaCl and other salt ions also have a significant effect on reducing bubble size (Pérez-Garibay et al., 2012). Bubble size can further be reduced by retarding coalescence due to surface-active agents (Azgomi et al., 2007). The effect and trend of frother concentration on bubble size is similar. At the low concentrations (below the critical coalescence concentration), the bubble size decreases significantly with increasing frother concentration, while this dependence of bubble size disappears at the higher concentrations (Finch et al., 2008; Gupta et al., 2007; Zhang, 2016). Increasing the liquid flow rate causes higher jet velocity and more impact strength between the jet fluid and tube wall. As a consequence, it is easier to break the bubbles into smaller ones (Zhang et al., 2020b). The pH of solutions (glucose, EDTA, DODAB, $Al3+$, $Fe3+$ or $Na+$) has variable impact on the bubble size. In some solution, pH has relatively small impacts (Bui et al., 2019). However, there is a consistent decreasing tendency for NB size with increasing pH value in solution (50 mg/L MIBC surfactant) using sodium hydroxide and hydrochloric acid to change the pH (Zhang et al., 2020b). With all other conditions equal, the size of NBs (using air, oxygen, ozone, and nitrogen) is also a function of gas solubility. Nitrogen with the lowest solubility generates the smallest bubbles, whereas ozone with highest solubility created the largest ones (Meegoda et al., 2018). There are other operational conditions affecting bubble size, such as the length, diameter, and type of hose (Temesgen et al., 2017).

5.2. Mass transfer efficiency

Mass transfer is the net movement of mass from one location to another caused by the existence of a certain driving force (e.g., uneven substance concentration) in the system (Ghassemi and Shahidian, 2017). The mass transfer process mainly includes the phenomenon of free diffusion of molecules in a laminar fluid and a stationary medium, vortex mixing and diffusion in a turbulent fluid, and mass transfer between gas and liquid phases. Based on Fick's law and two-film theory, the mass transfer efficiency is proportional to the overall mass transfer coefficient (including liquid and gas film coefficients), the specific area (surface area to volume ratio) and concentration gradient (the difference between the gas concentration in the liquid bulk phase and the gas saturation concentration in the liquid at the surface of the interface) (Droste, 1996; Parmar and Majumder, 2013). It is challenging to calculate the specific area. Therefore the volumetric mass transfer coefficient is mostly applied as an effective parameter representing the product of the overall mass transfer coefficient and specific area.

To be more precise, the bubble size, bubble rising velocity, specific area, mixing pattern, the reagents' (the chemicals, or solutes) physical properties all have essential impacts on the mass transfer efficiency. Using MBs with an average diameter of 110 μm, the volumetric mass transfer coefficient was raised by a factor of 100 with respect to other common bubbles made by open tube, needle, aquatic sparger or industrial sparger (Baker et al., 2016). Equation (1) was proposed to estimate the specific area (a) as a function of gas holdup (ε_g) and bubble diameter (d_b) (Chisti, 1989).

$$a = \frac{6\,\varepsilon_g}{\mathrm{d}_b} \tag{1}$$

It assumed that bubbles have a simple, spherical shape with one representative diameter and the gas holdup is dependent on the size of the bubble. Gas holdup (ε_g) is defined as the volume fraction occupied by the bubble or gas in the entire gas-liquid dispersion (Agarwal et al., 2011). Equation (1) states that the specific area tends to increase, when bubble size decreases or gas holdup increases. The surface area of MNBs is a significant factor determining the effectiveness of MNB technology in degrading contaminants as surface area relates to contaminant adsorption on the bubble surface (Yoshida et al., 2008). Gas holdup grows with frother concentration (Fig. 3) and has a close relationship with bubble size and velocity (Azgomi et al., 2007; Moyo et al., 2007). In the air-kerosene and air-water systems, gas holdup was found to depend on pressure and can be predicted by the dynamic gas disengagement method (Bae et al., 2020).

Owing to the decrease in surface tension and bubble coalescence reduction, the rising velocity of bubbles and liquid mass transfer coefficient decrease with an increasing salt concentration. The void fraction and volumetric mass transfer coefficient increase with superficial air velocity and salt concentration. Thus, the orders-of-magnitude increase in interfacial area at high salt concentrations is the main cause of the high volumetric mass transfer coefficient values (Kawahara et al., 2009). A theoretical model based on Epstein and Plesset theory expresses the mass transfer processes of oxygen and ozone MNBs in the contaminant treatment, describing the fate of MNBs and proving the benefits of MNBs over the traditional bubbles. The results showed that the increasing half-life of dissolved gas raises MNBs lifetime, but diminishes the MNB treatment impact. For gas with a long half-life and a slow consumption rate, the influence of half-life on the MNB life can be ignored (Epstein and Plesset, 1950; Xia and Hu, 2019a). An analytical model was applied to investigate the mass transfer and size change of a single bubble rising in stagnant water. It showed good prediction accuracy, considering the influence of changing dissolved gas concentration in the water and mass transfer across the water surface. The mass transfer efficiency is proportional to the bubble release depth, because of the longer bubble residence time and higher gas concentration gradient. This model can be applied to continuously injected bubble swarms (Li et al., 2020). Compared with coarse bubbles, aeration with NBs supplies more oxygen to aerobic biofilm systems, presenting a 1.5 times higher oxygen transfer efficiency at lower cost (Xiao and Xu, 2020). In order to further increase the mass transfer efficiency, gas agitation and/or ultrasound can be applied to MNB solutions to cause bubble oscillation (Zhao et al., 2018).

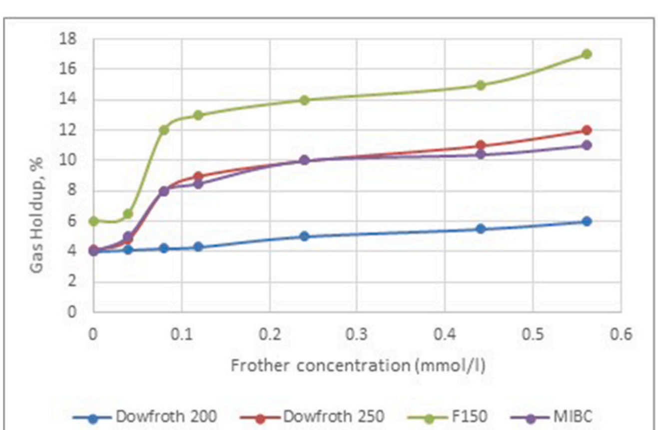

Fig. 3. Gas hold-up as a function of frother type and concentration. Figure adapted from (Azgomi et al., 2007) and (Moyo et al., 2007).

5.3. Bubble rising velocity

The behavior of the bubbles in water or other liquid solution is strongly influenced by a parameter known as rising velocity. The rising velocity of a MB through a liquid is determined by the balance of the buoyancy and drag forces acting on it. In water, the Reynolds number of MBs is well below unity, and the rising velocity (u) can be expressed by Stokes' law in terms of diameter of the bubble (d_b), density (ρ_l), and viscosity of the water (μ), as expressed in equation (2) (Stokes, 2009; Tanaka et al., 2020). Hadamard and Rybczynski developed Stokes theory to express the case of a bubble or fluid drop (Clift et al., 2005).

$$u = \frac{g d_b^2 \rho_l}{18\mu} \tag{2}$$

A bubbles swarm with a diameter of 2 mm had 10% higher rising velocity than a single bubble (Nock, 2015). With MBs generated by the pressurized dissolution method, experiments showed that liquid and gas properties have crucial impact on the terminal rising velocity of MBs (Parmar and Majumder, 2015). Theoretical also suggest important effects of gas molecular weight (i.e., CO_2, air, He, and N_2) on rising velocity (Parkinson et al., 2008). Azgomi et al. (2007) reported that a decrease in bubble rising velocity is strongly associated with a decrease in bubble size resulting in a continuous increase in gas holdup. In contaminated water, dispersed particles and fibers would adhere to MBs and decrease their rising velocity (Haapala et al., 2010). Compared with the vertical velocity, the bubble horizontal velocity has a small impact on mass transfer (Li et al., 2020). Surfactants are known to affect the rising velocity of bubbles. Their presence affects the surface tension on bubbles, which causes a tangential shear stress on the bubble surface and decreases the rising velocity. In the experiment of rising MBs in aqueous solutions of surfactant (SDS, Pluronic F68) or salt (NaCl), the MBs followed rectilinear trajectories in both contaminated and uncontaminated liquids, while the velocity of bubbles and drops were reduced by surfactants (Haapala et al., 2010; Tanaka et al., 2020). Due to the Brownian motion and low buoyancy forces, the MNBs rising velocity is small and, consequently, contributes to the stability of bubbles (Meegoda et al., 2018). The rising velocity of NBs has similar or lower magnitudes than Brownian motion (Li et al., 2014). The MB (50 μm −150 μm) rising velocity is not obviously different between saline water (0–44 mm/s) and freshwater (0–64 mm/s) (Fanaie and Khiadani, 2020). The terminal rising velocities of NBs, using a no-slip boundary condition, are 6.12 nm/s for a NB of radius equal to 50 nm and 612 nm/s for radius 500 nm, whereas the Brownian velocities are 3131 nm/s and 990 nm/s respectively. That means the Brownian motion dominates the NBs' behavior and against the impact of buoyancy (Alheshibri, 2019).

5.4. Zeta potential

Zeta potential is the electric potential difference between the mobile dispersion medium and the stationary layer of the dispersion medium adhered to the dispersed particle. Its value has a close relationship with short and long term stability of emulsions or colloids (Wei Lu and Ping, 2010). Zeta potential of MNBs describes the charge characteristics of MNBs, which affects their dispersion behavior. High absolute values of zeta potential were found to prevent MNBs from coalescence, thus, improving their stability (Hu and Xia, 2018). The electrophoretic light scattering technique is widely used to find the MNBs' zeta potential (Huang et al., 2020a; Weiner and Zhang, 2013; Xu, 2008). There are many factors exerting influences on the zeta potential of bubbles, such as pH of the solution, gas, ionic strength, concentration of additives, temperature, etc. (Wei Lu and Ping, 2010).

Zeta potential of NBs emerges from the capacity of the gas to create hydroxyl ions at the bubble surface. Solutions with high pH, low temperature and low salt concentrations facilitate high negative zeta potentials of bubbles. With time, the zeta potential of bubbles reduces in long term tests when the bubble size increase (Meegoda et al., 2018). A series of studies (Table 5) showed that it is difficult to compare exact value of zeta potentials for MNBs with a certain gas, as they use different methodologies; however, there are some overall tendencies (Kim et al., 2019). The zeta potential of MNBs are negative in the water without additives or reagents. For equal water conditions, the zeta potentials of MBs are similar and independent of their size. However, in the process of shrinkage of MBs, the gas-water interface traps some excess ions, which may increase the zeta potential. Hence, during MBs collapse, the zeta potential is negatively related to the bubble size (Takahashi et al., 2007a). The magnitude of negative surface charge of MNBs is proportional to the pH value. MNB zeta potential is always negative in wide pH range. At neutral pH, zeta potentials are negative (below −20 mV) for most gases. In an experiment using nonionic frother (MIBC), when the pH value rose from 3 to 12, the NB's size reduced from 652 nm to 251 nm and its zeta potential reduced from a positive value to – 9 mV. That is due to the electrostatic repulsion (Ulatowski et al., 2019; Zhang et al., 2020b). Negatively charged MBs can be generated by adding anionic surfactants like sodium dodecyl sulfate, whereas cationic surfactants like dodecyl amine hydrochloride, generate positively charged MBs. A similar trend was observed when MBs were coated with polymer flocculants. Negative charge was enhanced when the MB was coated with anionic polyacrylamide solution, while the charge changed from negative to positive when coated with cationic polyacrylamide solution (Parmar and Majumder, 2013). The absolute value of zeta potential shows an increasing trend when electrolyte (such as NaCl, $MgCl_2$) concentration increased, due to its impact on the diffuse double layer of NBs. Temperature has an inversely proportional effect on zeta potential, because higher temperatures enhance the mobility of ions and consequently reduce the hydroxyl ions attached on the bubble surface (Meegoda et al., 2018; Takahashi, 2005).

5.5. Transport of MNBs in porous media

The transport mechanism of MNBs in porous media has become a popular scientific topic, since it has dominant impact on the performance of soil and groundwater treatment. More insight of behavior of MNBs in soils can improve the remediation technologies based on MNBs (Hamamoto et al., 2017).

According to the geogas theory and Darcy's law, the velocity of MBs through dry porous media is proportional to the pressure gradient and permeability (Etiope and Lombardi, 1996). When the MBs move in water, there is always bubble coalescence. The nature of hydrodynamic boundary conditions at the gas-liquid interface, the hydrodynamic forces, attractive van der Waals-Lifshitz forces and bubble deformation exert an influence on bubble coalescence (Vakarelski et al., 2010).

The flow rate, gas species, particle size and pH value can influence the MNB transport in porous media. Lower flow rate in porous media increases the possibility of MNBs attachment in porous media. This phenomenon may be attributed to the smaller drag force and larger stagnant regions. At higher flow rates, the particle size of a porous medium has negligible impact on MNB transport (Hamamoto et al., 2016). Compared with larger sized MNBs, the smaller ones are more likely to retarded during transport (Hamamoto et al., 2017). Lower pH values increase the entrapment of NBs, because of the chemical heterogeneity on the solid surface and physical straining of bubbles. Besides, the reduced repulsive force between the solid and bubbles contributes to bubble attachment (Hamamoto et al., 2018). For the flow of discrete MBs through a water-saturated porous medium, the characteristic width and breakthrough time of bubble plumes were proportional to the gas release rate with power exponents of 0.2 and 0.4, while the cross-sectional averaged velocity of ambient pore water was related to the gas release rate with a power exponent of 0.6 (Ma et al., 2015).

5.6. Hydroxyl radical

In general, with continuous shrinkage of bubbles below 10 μm, the electric charge density of the double layer increases rapidly. When the bubble bursts in aqueous solutions, the positive and negative charges that have reached a very high concentration will instantly release the accumulated energy, producing many free radical ions, such as oxygen ions, hydrogen ions, hydroxide ions, etc. Among them, the hydroxyl radical has a strong oxidation effect, which can oxidize and decompose some difficult-to-degrade organic pollutants (such as phenol), and has a good effect in purifying water (Liu et al., 2012; Takahashi et al., 2007a). MNBs can generate free radicals without any dynamic stimulus or additives, but the free radicals are short-lived. Many studies explore the role of the free radicals in the water treatment. Experimental results show that the hydroxyl radical can be the major (82%) reactive oxidant species to degrade butylated hydroxytoluene (BHT) by ozone MNBs (Achar et al., 2020; Klammler et al., 2020; Kwon et al., 2020; Takahashi

Table 5
Zeta potential values reported in literature for different gases in water.

	Hasegawa et al. (2009) Ulatowski et al. (2019)		Ushikubo et al. (2010b) Hu and Xia (2018)		Meegoda et al. (2018)		Ushikubo et al. (2010a)	
Gas	Bubble size (nm)	Zeta potential (mV)	Bubble size (nm)	Zeta potential (mV)	Bubble size (nm)	Zeta potential (mV)	Bubble size (nm)	Zeta potential (mV)
Air		\	140 to 350	−20 to −17	20 to 204	−24.3 to −18.3	200 to 350	−20 to −17
O_2	\	\	137 to 380	−45 to −34	67 to 159	−25.8 to −19	200 to 350	−45 to −34
O_3	24,000 to 80000	−60 to −15	32 to 460	−23 to −18	86 to 210	−31.2 to −22.8	\	\
N_2	250 to 350	−15 to −10	\	\	38 to 166	−25.1 to −14.5	200 to 350	−35 to −29
CO_2	\	\	\	\	\	\	200 to 350	−27 to −20

et al., 2007a; Xiong et al., 2016).

The pH value and gas type have essential influence on the production of hydroxyl radicals by MNBs. It is well known that the elevated presence of hydroxide anions at high pH value is beneficial to the generation of hydroxyl radical. However, without accepted explanation today, experiments have also shown the opposite effect that strongly acidic conditions due to the addition of HCl, H_2SO_4, and HNO^{3-} accelerate the production of hydroxyl radicals. Furthermore, the gas type of MNBs also affects the quantity of free radicals created when MNBs burst (Li et al., 2009; Takahashi et al., 2007b; Xiong et al., 2016). Hydroxyl radical scavenger, such as sodium carbonate, in the solution have negative effects on contaminant removal due to its large consumption of hydroxyl radicals. In a laboratory batch experiment, after 80 s with 15, 25 and 30 mM of carbonate ions, the removal of BHT was decreased by 30%, 50% and 65% with respect to the same experiments conducted in the absence of carbonate ions (Achar et al., 2020; Jabesa and Ghosh, 2016). On the contrary, there are some kinds of catalysts, such as olive stone activated carbon, copper, MnO_2-coated Fe_3O_4, etc., which improve the generation of hydroxyl radicals. For example, adding olive stone activated carbon can accelerate the decomposition of ozone into hydroxyl radicals (Kang et al., 2019; Li et al., 2009; Rajah et al., 2019; Xiong et al., 2019).

6. Applications of MNBs in groundwater treatment

MNBs have caught a lot of attention recently in groundwater pollution control. This is due to their critical properties discussed above, such as huge surface area to volume ratio, high zeta potential, good mass transfer, etc. Particular methods involve air sparging to expel the volatile gases (Wang and Zhang, 2017), dissolved air floatation (Calgaroto et al., 2016, 2015; Ebrahimi et al., 2020; Etchepare et al., 2017; Oliveira et al., 2017), oxidation (Achar et al., 2020; Xia et al., 2019; Xia and Hu, 2019b) and disinfection (Cruz and Flores, 2017; Jhunkeaw et al., 2020; Saijai et al., 2019). Within these studies (Table 6), MNB with ozone are employed most frequently and possess a variety of existing or potential applications in groundwater remediation.

There is a wide variety of contaminants found in groundwater, including synthetic organic chemicals, hydrocarbons, inorganic cations, inorganic anions, pathogens, and radionuclides. These pollutants come from anthropogenic and natural pollution sources. The most common contamination sources are due to human activities, such as municipal solid waste disposal, use of fertilizer, pesticides and insecticides, industrial wastewater discharge, petroleum production, mining waste disposal, nuclear waste disposal, etc. (Fetter et al., 2017; Talabi and Kayode, 2019). All these activities may cause contaminants to infiltrate the subsurface. Hereby, not only the groundwater absorbs theses pollutants, but also the geologic formation retains residual contaminants. The latter usually lasts for a long time and becomes a persistent source for groundwater pollution.

Table 6
Overview of MNB applications.

Num	Contaminant				MNB			Author and year
	Type	Initial concentration	Reaction time	Removal rate (%)	Size	Gas/ additive	Working conditions	
1	methyl orange	50 mg/L	50 min	100	265 nm	ozone	reaction tank 20 L in lab, 20 °C	,Xia and Hu (2019b)
2	methyl orange	10 mg/L	30 min	98.2	247 nm	ozone	colume test: 0.12 m diameter, 0.76 m high, glass beads	Hu and Xia (2018)
3	methyl orange	10 mg/L	30 min	1	247 nm	oxygen	colume test: 0.12 m diameter, 0.76 m high, glass beads	Hu and Xia (2018)
4	methyl orange	10 mg/L	2 h	99	\	ozone	colume test: 0.1 m diameter, 0.15 m high, sandy soil	Liu et al. (2018)
5	Industrial wastewater (COD)	4500 mg/L	14 h	63	266 nm	ozone	reaction tank 20 L in lab, 21 °C, pH 9.9, high salinity	Xia and Hu (2019b)
6	Contaminated Groundwater	Benzene (31); Chlorobenzene (15); Nitrobenzene (503); p (0)-nitrochlorobenzene (10), mg/L	30 min	Benzene (98); Chlorobenzene (97); Nitrobenzene (67); p (0)-nitrochlorobenzene (35)	267 nm	ozone	reaction tank 20 L in lab, 22 °C, pH 6.7	Xia and Hu (2019b)
7	Trichloroethylene (TCE)	10 mg/L	6 days; 9 h/day	99	247 nm	ozone; H_2O_2	field test in an organics contaminanted site; 6.5 m below the ground surface; sandy aquifer (hydraulic conductivity 10−6 m/s)	Xia et al. (2019)
8	Nitrogen	40 mg/L	24 h	99	25 μm	hydrogen	laboratory-scale cylindrical reactor with Enriched hydrogenotrophic denitrification (HD) sludge (microbial community), 32 °C.	Eamrat et al. (2020)
9	petroleum hydrocarbons	8000 mg/kg	120 min	70.9	220 nm-50 μm	ozone	0.04 m diameter, 0.7 m high column with oily sludge;	Sun et al. (2020)
10	Butylated hydroxytoluene (BHT)	0.9 μM	60 s	77	14.64 μm	ozone	a batch type reactor 16 L, flow rate of bubble generator 75 L/min; ozone flow rate 1 L/min	Achar et al. (2020)
11	n-Decane	3.3 mL	72 h	42	4.9 μm	ozone	a glass column (15 cm × 2.5 cm) with glass beads, gas flow rate of 2.0 mL/min	Kwon et al. (2020)
12	copper nitrate	500 ppm	6 h	18.48	171 nm	Hydrogen	the batch test with soil (sand), solid–liquid ratio 1:20	Kim and Han (2020)

6.1. Degradation of organic pollutants in groundwater

With the economic development related to oil extraction, agriculture, wastewater discharge, waste disposal and respective leakage events, organic substances, such as petroleum hydrocarbons, organic chlorides and organic nitrogen, have become major groundwater pollutants. MNB technique can enhance the bioremediation and oxidation in groundwater to degrade the pollutants to non-harmful or less toxic materials (Al-Raoush et al., 2018; El Alfy et al., 2017; Pérez-Lucas et al., 2019; Talabi and Kayode, 2019). Pump and treat is one of the traditional groundwater remediation technologies and can be applied with the MNB technique (Li et al., 2015).

Ammonia widely exists in the aqueous environment due to domestic and industrial wastewater and consumes dissolved oxygen in the water. Oxidation is one of the most common ways to remove ammonia. Compared with other methods, such as biological denitrification, air stripping or chlorination, oxidation does not imply a complex series of denitrification reactions, avoids air pollution and chlorine residuals, and does not depend on the cultivation of bacteria. In a pilot plant, ozonation of ammonia using MB was very effective and superior to that of oxygen MBs. Ammonia is oxidized faster in higher pH or with catalyst (bromide ions) (Khuntia et al., 2013). In pilot-scale tests, ozone MBs were applied to the continuous flow (one synthetic and one real mine effluent) to remove the ammonia. The ammonia removal rate was up to 99.1% at a flow rate of 1.1 L/min over 570 min. That demonstrated the feasibility of larger-scale treatment with ozone MBs (Ryskie et al., 2020). Wang and Zhang studied the nitrogen removal efficiency and mechanism of deep subsurface wastewater infiltration systems by MNBs. A total nitrogen removal efficiency of 85.4% was achieved by circulating MNB solution in the soil column saturated with simulated livestock wastewater (Wang and Zhang, 2017).

Synthetic phenolic antioxidants (SPAs) are the predominant plastic additives in our daily life and impose an environmental risk on surface water and groundwater due to their high industrial production, large-scale applications, and toxicity. Butylated hydroxytoluene (BHT) is one of the SPAs family and ubiquitous in nature. From experiments conducted in a batch type reactor, ozone MBs were found to degrade BHT and reduce its toxicity. It was shown that the OH created from ozone in water was the key (82%) reactive oxidant species for the complete degradation of BHT using zone MBs (Achar et al., 2020; Hahladakis et al., 2018). In the oil production areas, exposure to petroleum hydrocarbons (TPH) is well known to deteriorate the quality of groundwater. In laboratory experiments, MB ozonation was used to enhance the efficiency of TPH removal in sludge sample from a Shanghai oil refinery. The research indicated that 70.9% of TPH could be degraded into more readily biodegradable intermediate products from oily sludge in 120 min, with pH of 3, ozone dosage of 0.27 g O_3/g TS and total solid of 2%. Being a green technology, ozone MBs converted more heavy hydrocarbons to light fractions compared with macrobubble ozonation (Sun et al., 2020). Physical adsorption is not suitable for wastewater containing multiple pollutants, and biological techniques are time consuming and greatly affected by the ambient conditions. Studies found that ozone MNBs were able to remediate contaminated groundwater with complex organic components, even in the presence of high salinity concentration to which physical adsorption and biological methods are inefficient. Ozone MNBs had a remarkable performance for degradation of persistent organic contaminants, such as benzene and chlorobenzene, after 30 min of treatment (Xia and Hu, 2019b). Numerous applications using the MNBs with ozone to remove other organic pollutants (methyl orange, COD, etc.) were conducted and showed that ozone MNBs have great prospect in groundwater treatment (Hu and Xia, 2018, 2018; Ikeura et al., 2011; Kwon et al., 2020; Nam et al., 2019; Takahashi et al., 2012; Zheng et al., 2015).

In reality, there are many kinds of impurities or contaminants in polluted groundwater at the same time. Mine effluents, for example, contain cyanides, cyanate, thiocyanate, and metals, the mixture of which has adverse impact on treatment efficiency. Except for organic pollutants, groundwater quality may be impacted by inorganic contaminants, such as heavy metals or nitrate, for example. For these conditions, MNBs with hydrogen may facilitate partial remediation (Eamrat et al., 2020; Kim and Han, 2020).

6.2. Pollutant removal in porous media

Thanks to large specific surface area, long retention time and high oxygen transfer efficiency, MNBs filled with air or oxygen improve the availability of dissolved oxygen in groundwater and as a result, have a positive effect on the growth of aerobic microorganism. One kind of the enhanced bioremediation uses a specific microorganism to absorb, transform or degrade contaminations in porous media. With the improved environmental conditions, the growth and metabolism of microorganisms accelerate the degradation of harmful substances to reduce or eliminate groundwater pollution (Fetter et al., 2017; KIM et al., 2016; Li et al., 2015, 2013b).

As a carrier of oxygen, MB suspension, which consisted of saponin, not only delivered oxygen, but also transported microorganisms, and micronutrients to the target area where environmental factors are limited. In the batch scale study, the saponin-MBs in the retarded gas front helped bacteria to degrade about 30% of phenanthrene in 21 days (Park et al., 2009). Saponin based MBs successfully improved the aerobic biodegradation potential of organic pollutants in sand under an oxygen-limiting environment (Choi et al., 2009). The effect of surfactant solution and surfactant MB on bacteria transport in sand columns were also studied. Results show that bacterial hydrophobicity was changed due to the different surfactant but sand particles' hydrophobicity did not alter for different surfactant. A continuous supply of MBs can transport bacteria into the soil using a smaller quantity of surfactant. Higher porosity facilitates bacterial movement significantly in porous media (Tao, 2018).

Oil spill-contaminated sands can be treated by the self-collapsing MBs-based method. Related research demonstrated that MBs created in tap water removed almost all oils from the polluted sands in 40 min while in saline water it decreased to 90%. Because of the susceptibility of MBs to shrink in size, when they finally collapse, a high-pressure spot develops and causes pressure waves. These pressure waves remove the oil form the sand grain surface. Air MBs (smaller than 50 μm) showed more advantages compared with the other biological, chemical and physical methods in terms of remediation efficiency and environmental protection (Agarwal et al., 2016; Sun et al., 2019). In order to enhance the cleaning efficacy of MBs, low intensity, pulsed ultrasound, high salinity and high temperature can be applied to diesel contaminated fine and medium sands (Agarwal and Liu, 2017).

Besides bioremediation and physical removal, oxidation is another important method to remediate groundwater pollution. As mentioned above, ozone MNBs are a powerful oxidation technology and has received growing attention in recent years. In most studies, methyl orange was chosen as representative organic pollutants in the experiments, due to its high visibility, low cost, and similarity to real organic contaminants. In experiments, different sizes of sandy soil are used, including 35–50, 70–100,150-200 and 200–300 meshes. In the sandy soil column contaminated by 10 mg/L methyl orange, ozone MNBs achieved a removel rate of 99%, showing an excellent cleaning performance (Liu et al., 2018). Hu and Xia (2018) also conducted a column test made of glass beads and use ozone MNBs to decompose methyl orange. As opposed to oxygen MNBs, ozone MNBs can oxidize methyl orange. This means that free radicals created from the MNB collapse have little effect on the removal of methyl orange. Furthermore, in field tests at a TCE-contaminate site using ozone MNBs, the TCE concentration in the monitoring wells diminished significantly and the final removal rate reached 99% after 6 days. Compared with ozone MNBs and H_2O_2, the ozone MNBs plus H_2O_2 achieved the remediation target more quickly. Although H_2O_2 alone had low treatment efficacy for TCE, it enhanced the ozone MNB efficiency by a factor of 3 (Hu and Xia, 2018). Kwon et al. (2020) deployed decane as the representative NAPL and oil-soluble fluorescence as tracer in bench-scale experiments. Different combinations of treatments, such as ozone sparging, air MNB solution flushing, ozone MNB solution flushing, and ozone MNB solution flushing plus H_2O_2, are conducted and compared regarding the effect of hydroxyl free radicals on NAPL removal. The results indicate that H_2O_2 helped the ozone MNBs increase the NAPL removal by 22% and oxidative degradation of NAPL only happened on the NAPL-water interface owing to the reactivity of hydroxyl free radical when ozone MNB plus H_2O_2 are applied. According to the end products of different treatment types, the removal mechanisms depends on the oxidation agent and the state of oxidizing fluid (Kwon et al., 2020). In addition, MNBs are able to remediate the heavy metal-contaminated soil. Due to the large surface area and high zeta potential, NBs water has better removal rates than distilled water regardless of soil type (Jeong et al., 2017).

7. Challenges and limitations of MNBs

Growing knowledge over the past decades gradually contributes to unveiling the mystery of MNBs, thus preparing the stage for use of MNB techniques to solve various engineering problems, including groundwater treatment. However, after this review of recent scientific contributions on MNBs properties and applications, there are still significant challenges and limitations on the path to routine field/industrial implementations.

(1) Even though many laboratory studies showed great potential of MNB in water treatment, there is little knowledge regarding the upscaling of methods and application of MNB at the industrial level. Therefore, more field size experiments should be conducted for longer periods to evaluate efficiency and get the operational experience.
(2) A variety of techniques exist for MNB generation, but bubble size and concentration are typically unstable and heterogeneous. This hinders a deeper exploration of bulk MNB properties, since it is hard to discern, what portion of the bubbles contribute more to water treatment efficacy.
(3) Many other characteristics of MNB-liquid are unknown and explored, such as heat transfer, viscosity and hydraulic conductivity. The high mass transfer efficiency is usually highlighted in a great number of studies, while very few reveal other properties. Heat transfer of MNB is as important as the mass transfer, since all bubble generators inevitably generate heat, and temperature is a key factor for physical, biological, and chemical processes. The hydraulic conductivity of porous media with respect to groundwater flow is highly affected by the presence of MNBs and plays a vital role in pollution control.
(4) Modeling approaches of MNBs generation, stability and reaction with pollutants are rare (Klammler et al., 2020). Modeling can help people to simulate and get better understanding about the MNB-induced processes without experiments. It can greatly reduce the design and operation cost when used for optimizing the process. In addition, theoretical MNB studies barely take the porous media into consideration. Improved models for transport, chemical transformation and mass transfer coupled with porous media are needed.
(5) The synergistic and antagonistic interaction with microbial activities during application of MNB techniques are unknown. Many studies in the laboratory and some in the field have been conducted and confirmed the good effect on groundwater remediation due to the bioremediation and oxidation; however, there are many other kinds of microorganism, which do not contribute the remediation but are important to local ecosystem. MNB influence imposed on them is uncovered. During treatment, the groundwater containing MNBs filled with oxygen or ozone definitely affect the original organism underground which is the key player in local ecosystem. Because the polluted groundwater always needs a long treatment period, the long-term effect of MNB should be studied as well. How the MNBs change the water environment, how far the MNB transport and how the other microorganism interact with MNB are essential for the MNB application.
(6) A comprehensive cost-benefit analysis approach is required. Even if MNB technologies are highly effective and environmentally friendly, the development and practical application will be restricted if the cost-benefit is high. Some investigations indicated MNB has lower cost than other methods (Rizaldi et al., 2019; Vion, 2007), but there is not sufficient data for reliable quantification. A comprehensive cost-benefit analysis should cover the whole life of the MNB treatment system, including the design, construction, training, maintenance, operation, disposal, etc. Moreover, economic, social and environmental analyses should be involved.

8. Conclusions

MNBs are a promising technology that can be applied to enhance treatment effects in groundwater remediation. This technology does not require complex treatment facilities and hence it has low design and operational cost, compared to other physical and chemical remediation techniques. Shorter treatment period is required as MNBs increase the metabolism and enhance the bioremediation. This technology consumes fewer chemicals and has a smaller adverse impact on ecosystems. In this regard, MNB technology is sustainable and its application has significant importance for future groundwater treatment because of MNBs' excellent mass transfer efficiency, high zeta potential, relatively low rising velocity, and stronger free radical generation ability. However, there are numerous challenges and limitations remaining for future research.

Declaration of competing interest

The authors declare that they have no known competing financial interests or personal relationships that could have appeared to influence the work reported in this paper.

Acknowledgements

This work was supported by funding from the United Arab Emirates University National Water Center (Grant No. 31R112).

References

Achaoui, Y., Metwally, K., Fouan, D., Hammadi, Z., Morin, R., Debieu, E., Payan, C., Mensah, S., 2017. Tunable microbubble generator using electrolysis and ultrasound. AIP Adv. 7, 015011 https://doi.org/10.1063/1.4973720.
Achar, J.C., Nam, G., Jung, J., Klammler, H., Mohamed, M.M., 2020. Microbubble ozonation of the antioxidant butylated hydroxytoluene: degradation kinetics and toxicity reduction. Environ. Res. 186, 109496. https://doi.org/10.1016/j.envres.2020.109496.
Agarwal, A., Liu, Y., 2017. Enhanced microbubbles assisted cleaning of diesel contaminated sand. Mar. Pollut. Bull. 124, 331–335. https://doi.org/10.1016/j.marpolbul.2017.07.041.
Agarwal, A., Ng, W.J., Liu, Y., 2011. Principle and applications of microbubble and nanobubble technology for water treatment. Chemosphere 84, 1175–1180. https://doi.org/10.1016/j.chemosphere.2011.05.054.
Agarwal, A., Zhou, Y., Liu, Y., 2016. Remediation of oil-contaminated sand with self-collapsing air microbubbles. Environ. Sci. Pollut. Res. 23, 23876–23883. https://doi.org/10.1007/s11356-016-7601-5.
Aghdam, A.S., Ghorbani, M., Deprem, G., Cebeci, F.Ç., Koşar, A., 2019. A new method for intense cavitation bubble generation on layer-by-layer assembled SLIPS. Sci. Rep. 9, 11600. https://doi.org/10.1038/s41598-019-48175-4.
Ahrer, K., Buchacher, A., Iberer, G., Josic, D., Jungbauer, A., 2003. Analysis of aggregates of human immunoglobulin G using size-exclusion chromatography, static and dynamic light scattering. Journal of chromatography A 1009, 89–96.
Al-Raoush, R., Ngueleu, S., Rezanezhad, F., Cappellen, P.V., 2018. Groundwater pollution by petroleumderived contaminants in coastal semiarid environment. In: Presented at the Qatar Foundation Annual Research Conference Proceedings, vol.

2018. Hamad bin Khalifa University Press (HBKU Press, p. EEPD709. https://doi.org/10.5339/qfarc.2018.EEPD709. Issue 1.

Alam, R., Shang, J.Q., Khan, A.H., 2017. Bubble size distribution in a laboratory-scale electroflotation study. Environ. Monit. Assess. 189, 193. https://doi.org/10.1007/s10661-017-5888-4.

Alheshibri, M.H., 2019. Nanobubbles in Bulk.

Alheshibri, M., Craig, V.S.J., 2019. Generation of nanoparticles upon mixing ethanol and water; Nanobubbles or Not? J. Colloid Interface Sci. 542, 136–143. https://doi.org/10.1016/j.jcis.2019.01.134.

Alheshibri, M., Qian, J., Jehannin, M., Craig, V.S.J., 2016. A history of nanobubbles. Langmuir 32, 11086–11100. https://doi.org/10.1021/acs.langmuir.6b02489.

Atkinson, A.J., Apul, O.G., Schneider, O., Garcia-Segura, S., Westerhoff, P., 2019. Nanobubble technologies offer opportunities to improve water treatment. Acc. Chem. Res. 52, 1196–1205. https://doi.org/10.1021/acs.accounts.8b00606.

Azevedo, A., Oliveira, H., Rubio, J., 2019. Bulk nanobubbles in the mineral and environmental areas: updating research and applications. Adv. Colloid Interface Sci. 271, 101992. https://doi.org/10.1016/j.cis.2019.101992.

Azgomi, F., Gomez, C.O., Finch, J.A., 2007. Correspondence of gas holdup and bubble size in presence of different frothers. Int. J. Miner. Process. 83, 1–11. https://doi.org/10.1016/j.minpro.2007.03.002.

Bae, K., Go, G.S., Noh, N.S., Lim, Y.-I., Bae, J., Lee, D.H., 2020. Bubble characteristics in pressurized bubble column associated with micro-bubble dispersion. Chem. Eng. J. 386, 121339. https://doi.org/10.1016/j.cej.2019.03.215.

Baker, J.J., Crivellari, F., Gagnon, Z., Betenbaugh, M.J., 2016. Microfluidic bubbler facilitates near complete mass transfer for sustainable multiphase and microbial processing. Biotechnol. Bioeng. 113, 1924–1933. https://doi.org/10.1002/bit.25972.

Beekers, I., Mastik, F., Beurskens, R., Tang, P.Y., Vegter, M., van der Steen, A.F.W., de Jong, N., Verweij, M.D., Kooiman, K., 2020. High-resolution imaging of intracellular calcium fluctuations caused by oscillating microbubbles. Ultrasound Med. Biol. https://doi.org/10.1016/j.ultrasmedbio.2020.03.029.

Bui, T.T., Nguyen, D.C., Han, M., 2019. Average size and zeta potential of nanobubbles in different reagent solutions. J. Nano Res. 21, 173. https://doi.org/10.1007/s11051-019-4618-y.

Calgaroto, S., Azevedo, A., Rubio, J., 2015. Flotation of quartz particles assisted by nanobubbles. Int. J. Miner. Process. 137, 64–70. https://doi.org/10.1016/j.minpro.2015.02.010.

Calgaroto, S., Azevedo, A., Rubio, J., 2016. Separation of amine-insoluble species by flotation with nano and microbubbles. Miner. Eng. 89, 24–29. https://doi.org/10.1016/j.mineng.2016.01.006.

Chen, Z., Li, S., Han, G., Xie, Y., 2008. Miro-bubble pure oxygen aeration for sewage disposal in methanol plant. M-sized Nitrogenous Fertilizer Progress 8–12.

Chisti, M.Y., 1989. Airlift Bioreactors, Elsevier Applied Biotechnology Series. Elsevier Applied Science, London.

Choi, Y.J., Kim, Y.-J., Nam, K., 2009. Enhancement of aerobic biodegradation in an oxygen-limiting environment using a saponin-based microbubble suspension. Environ. Pollut. 157, 2197–2202. https://doi.org/10.1016/j.envpol.2009.04.014.

Clift, R., Grace, J.R., Weber, M.E., 2005. Bubbles, Drops, and Particles. Courier Corporation.

Clogston, J.D., Patri, A.K., 2011. Zeta potential measurement. In: McNeil, S.E. (Ed.), Characterization of Nanoparticles Intended for Drug Delivery, Methods in Molecular Biology. Humana Press, Totowa, NJ, pp. 63–70. https://doi.org/10.1007/978-1-60327-198-1_6.

Cruz, R., Flores, J.V., 2017. Reduction of coliforms presents in domestic residual waters by air-ozone micro-nanobubbles in Carhuaz city, Perú. Journal of Nanotechnology 1, 9–17.

Daryabor, M., Ahmadi, A., Zilouei, H., 2017. Solvent extraction of cadmium and zinc from sulphate solutions: comparison of mechanical agitation and ultrasonic irradiation. Ultrason. Sonochem. 34, 931–937. https://doi.org/10.1016/j.ultsonch.2016.07.014.

Droste, R.L., 1996. Theory and Practice of Water and Wastewater Treatment. John Wiley & Sons Inc, New York.

Eamrat, R., Tsutsumi, Y., Kamei, T., Khanichaidecha, W., Ito, T., Kazama, F., 2020. Microbubble application to enhance hydrogenotrophic denitrification for groundwater treatment. Environment and Natural Resources Journal 18, 156–165.

Ebrahimi, H., Karamoozian, M., Saghravani, S.F., 2020. Interaction of applying stable micro-nano bubbles and ultrasonic irradiation in coal flotation. International Journal of Coal Preparation and Utilization 1–15. https://doi.org/10.1080/19392699.2020.1732947.

El Alfy, M., Lashin, A., Abdalla, F., Al-Bassam, A., 2017. Assessing the hydrogeochemical processes affecting groundwater pollution in arid areas using an integration of geochemical equilibrium and multivariate statistical techniques. Environ. Pollut. 229, 760–770. https://doi.org/10.1016/j.envpol.2017.05.052.

Elserwy, A.A., 2019. Removal of Pollutants from Potable Water by Aeration. Water Technology Experts Forum 12.1.19 ,منتدى خبراء تكنولوجيا المياه. https://watertechexperts.com/removal-of-pollutants-from-potable-water-by-aeration/.

Epstein, P.S., Plesset, M.S., 1950. On the stability of gas bubbles in liquid-gas solutions. J. Chem. Phys. 18, 1505–1509. https://doi.org/10.1063/1.1747520.

Etchepare, R., Azevedo, A., Calgaroto, S., Rubio, J., 2017. Removal of ferric hydroxide by flotation with micro and nanobubbles. Separ. Purif. Technol. 184, 347–353. https://doi.org/10.1016/j.seppur.2017.05.014.

Etiope, G., Lombardi, S., 1996. Laboratory simulation of geogas microbubble flow. Geo 27, 226–232. https://doi.org/10.1007/BF00770436.

Fales, A.M., Vogt, W.C., Wear, K.A., Pfefer, T.J., Ilev, I.K., 2019. Experimental investigation of parameters influencing plasmonic nanoparticle-mediated bubble generation with nanosecond laser pulses. JBO 24, 065003. https://doi.org/10.1117/1.JBO.24.6.065003.

Fan, W., An, W., Huo, M., Yang, W., Zhu, S., Lin, S., 2020. Solubilization and stabilization for prolonged reactivity of ozone using micro-nano bubbles and ozone-saturated solvent: a promising enhancement for ozonation. Separ. Purif. Technol. 238, 116484. https://doi.org/10.1016/j.seppur.2019.116484.

Fanaie, V.R., Khiadani, M., 2020. Effect of salinity on air dissolution, size distribution of microbubbles, and hydrodynamics of a dissolved air flotation (DAF) system. Colloid. Surface. Physicochem. Eng. Aspect. 591, 124547. https://doi.org/10.1016/j.colsurfa.2020.124547.

Fetter, C.W., Boving, T., Kreamer, D., 2017. Contaminant Hydrogeology, third ed. Waveland Press.

Finch, J.A., Nesset, J.E., Acuña, C., 2008. Role of frother on bubble production and behaviour in flotation. Miner. Eng. xxxx 21, 949–957. https://doi.org/10.1016/j.mineng.2008.04.006.

Geisse, N.A., 2009. AFM and combined optical techniques. Mater. Today 12, 40–45. https://doi.org/10.1016/S1369-7021(09)70201-9.

Ghassemi, M., Shahidian, A., 2017. Nano and Bio Heat Transfer and Fluid Flow. Academic Press, an imprint of Elsevier, London.

Griffiths, D., Carnell-Morris, P., Wright, M., 2020. Nanoparticle tracking analysis for multiparameter characterization and counting of nanoparticle suspensions. In: Ferrari, E., Soloviev, M. (Eds.), Nanoparticles in Biology and Medicine: Methods and Protocols, Methods in Molecular Biology. Springer US, New York, NY, pp. 289–303. https://doi.org/10.1007/978-1-0716-0319-2_22.

Guo, W., Liu, J., Liu, J., Wang, G., Wang, G., Huang, M., 2019. A single-ended ultra-thin spherical microbubble based on the improved critical-state pressure-assisted arc discharge method. Coatings 9, 144. https://doi.org/10.3390/coatings9020144.

Gupta, A.K., Banerjee, P.K., Mishra, A., Satish, P., 2007. Effect of alcohol and polyglycol ether frothers on foam stability, bubble size and coal flotation. Int. J. Miner. Process. 82, 126–137.

Haapala, A., Honkanen, M., Liimatainen, H., Stoor, T., Niinimäki, J., 2010. Hydrodynamic drag and rise velocity of microbubbles in papermaking process waters. Chem. Eng. J. 162, 956–964. https://doi.org/10.1016/j.cej.2010.07.001.

Hahladakis, J.N., Velis, C.A., Weber, R., Iacovidou, E., Purnell, P., 2018. An overview of chemical additives present in plastics: migration, release, fate and environmental impact during their use, disposal and recycling. J. Hazard Mater. 344, 179–199. https://doi.org/10.1016/j.jhazmat.2017.10.014.

Hain, N., Handschuh-Wang, S., Wesner, D., Druzhinin, S.I., Schönherr, H., 2019. Multimodal microscopy-based identification of surface nanobubbles. J. Colloid Interface Sci. 547, 162–170. https://doi.org/10.1016/j.jcis.2019.03.084.

Hamamoto, S., Nihei, N., Ueda, Y., Moldrup, P., Nishimura, T., 2016. Effects of particle size and bubble characteristics on transport of micro- and nano-bubbles in saturated porous media. In: AGU Fall Meeting Abstracts, vol. 33.

Hamamoto, S., Nihei, N., Ueda, Y., Moldrup, P., Nishimura, T., 2017. Effects of flow rate and gas species on microbubble and nanobubble transport in porous media. J. Environ. Eng. 143, 04017023 https://doi.org/10.1061/(ASCE)EE.1943-7870.0001216.

Hamamoto, S., Takemura, T., Suzuki, K., Nishimura, T., 2018. Effects of pH on nano-bubble stability and transport in saturated porous media. J. Contam. Hydrol. 208, 61–67. https://doi.org/10.1016/j.jconhyd.2017.12.001.

Hasegawa, H., Kataoka, H., Asano, K., 2009. Effect of electrical potential of microbubbles on ozone dissolution. J. Phys.: Conf. Ser. 147, 012024 https://doi.org/10.1088/1742-6596/147/1/012024.

Hong, H., Woo, S., Ahn, S., Kim, J., Oh, S., Lee, J., Hwang, M., 2020. Microbubble Generating System. US20200078745A1.

Hu, L., Xia, Z., 2018. Application of ozone micro-nano-bubbles to groundwater remediation. J. Hazard Mater. 342, 446–453. https://doi.org/10.1016/j.jhazmat.2017.08.030.

Hu, L., Wu, X., Liu, Y., Meegoda, J.N., Gao, S., 2010. Physical modeling of air flow during air sparging remediation. Environ. Sci. Technol. 44, 3883–3888. https://doi.org/10.1021/es903853v.

Huang, G., Xu, B., Qiu, J., Peng, L., Luo, K., Liu, D., Han, P., 2020a. Symmetric electrophoretic light scattering for determination of the zeta potential of colloidal systems. Colloid. Surface. Physicochem. Eng. Aspect. 587, 124339. https://doi.org/10.1016/j.colsurfa.2019.124339.

Huang, J., Sun, L., Liu, H., Mo, Z., Tang, J., Xie, G., Du, M., 2020b. A review on bubble generation and transportation in Venturi-type bubble generators. Exp. Comput. Multiph. Flow 2, 123–134. https://doi.org/10.1007/s42757-019-0049-3.

Huang, X., Li, Z., Deng, Y., Cai, W., Gu, L., Lu, H., 2020c. Effect of micro- and nanobubbles on the crystallization of THF hydrate based on the observation by atomic force microscopy. J. Phys. Chem. C. https://doi.org/10.1021/acs.jpcc.0c00181.

Huszka, G., Gijs, M.A.M., 2019. Super-resolution optical imaging: a comparison. Micro and Nano Engineering 2, 7–28. https://doi.org/10.1016/j.mne.2018.11.005.

Ikeura, H., Kobayashi, F., Tamaki, M., 2011. Removal of residual pesticides in vegetables using ozone microbubbles. J. Hazard Mater. 186, 956–959. https://doi.org/10.1016/j.jhazmat.2010.11.094.

Interstate Technology, Regulatory Council, 2005. Overview of Groundwater Remediation Technologies for MTBE and TBA 1–94.

Jabesa, A., Ghosh, P., 2016. Removal of diethyl phthalate from water by ozone microbubbles in a pilot plant. J. Environ. Manag. 180, 476–484. https://doi.org/10.1016/j.jenvman.2016.05.072.

Jabra Shnoudeh, A., Hamad, I., Alkelany, S.Z., 2019. Biomaterials and Bionanotechnology-Chapter 15 - Synthesis, Characterization, and Applications of Metal Nanoparticles. Elsevier. https://doi.org/10.1016/C2017-0-01066-2.

Jadhav, A.J., Barigou, M., 2020. Bulk nanobubbles or not nanobubbles: that is the question. Langmuir 36, 1699–1708. https://doi.org/10.1021/acs.langmuir.9b03532.
Jeong, S.-H., Kim, D.-C., Han, J.-G., 2017. The Fundamental Study on th e Soil Remediation for Copper Contaminated Soil using Nanobubble Water. Journal of the Korean Geosynthetics Society 16, 31–39. https://doi.org/10.12814/jkgss.2017.16.1.031.
Jhunkeaw, C., Khongcharoen, N., Rungrueng, N., Sangpo, P., Panphut, W., Thapinta, A., Senapin, S., St-Hilaire, S., Dong, H.T., 2020. Ozone Nanobubble Treatment Effectively Reduced Pathogenic Gram Positive and Negative Bacteria in Freshwater and Safe for tilapia. bioRxiv.
Jiang, H., Wu, T., 2011. The application of micro-nano-aeration technology in water envrionment treatment. Hehai Water conservancy 24–26.
Jin, J., Feng, Z., Yang, F., Gu, N., 2019. Bulk nanobubbles fabricated by repeated compression of microbubbles. Langmuir 35, 4238–4245. https://doi.org/10.1021/acs.langmuir.8b04314.
Jin, J., Wang, R., Tang, J., Yang, L., Feng, Z., Xu, C., Yang, F., Gu, N., 2020. Dynamic tracking of bulk nanobubbles from microbubbles shrinkage to collapse. Colloid. Surface. Physicochem. Eng. Aspect. 589, 124430. https://doi.org/10.1016/j.colsurfa.2020.124430.
Juwana, W.E., Widyatama, A., Majid, A.I., Wiratni, Indarto, Deendarlianto, 2018. The application of digital image analysis to study the characteristic of bubble size distribution produced by orifice type microbubble generator. In: AIP Conference Proceedings 2001, 050004. https://doi.org/10.1063/1.5049995.
Juwana, W.E., Widyatama, A., Dinaryanto, O., Budhijanto, W., Indarto, Deendarlianto, 2019. Hydrodynamic characteristics of the microbubble dissolution in liquid using orifice type microbubble generator. Chem. Eng. Res. Des. 141, 436–448. https://doi.org/10.1016/j.cherd.2018.11.017.
Kang, Y.-G., Yoon, H., Lee, C.-S., Kim, E.-J., Chang, Y.-S., 2019. Advanced oxidation and adsorptive bubble separation of dyes using MnO2-coated Fe3O4 nanocomposite. Water Res. 151, 413–422. https://doi.org/10.1016/j.watres.2018.12.038.
Kawahara, A., Sadatomi, M., Matsuyama, F., Matsuura, H., Tominaga, M., Noguchi, M., 2009. Prediction of micro-bubble dissolution characteristics in water and seawater. Exp. Therm. Fluid Sci. 33, 883–894. https://doi.org/10.1016/j.expthermflusci.2009.03.004.
Khuntia, S., Majumder, S.K., Ghosh, P., 2012. Microbubble-aided water and wastewater purification: a review. Rev. Chem. Eng. 28, 191–221. https://doi.org/10.1515/revce-2012-0007.
Khuntia, S., Majumder, S.K., Ghosh, P., 2013. Removal of ammonia from water by ozone microbubbles. Ind. Eng. Chem. Res. 52, 318–326. https://doi.org/10.1021/ie302212p.
Kim, D., Han, J., 2020. Remediation of copper contaminated soils using water containing hydrogen nanobubbles. Appl. Sci. 10, 2185. https://doi.org/10.3390/app10062185.
Kim, T. il, Kim, Y. ha, Han, M., 2012. Development of novel oil washing process using bubble potential energy. Mar. Pollut. Bull. 64, 2325–2332. https://doi.org/10.1016/j.marpolbul.2012.08.031.
Kim, E., Jung, J., Kang, S., Choi, Y., 2016. Characterization of nano-bubbles as an oxygen carrier for in-situ bioremediation of organic pollutants in the subsurface. AGU Fall Meeting Abstracts 31.
Kim, S., Kim, H., Han, M., Kim, T., 2018. Verifying sub-micron (nano) bubbles generation and their fundamental characteristics. Environmental Engineering Research 24. https://doi.org/10.4491/eer.2018.210.
Kim, S., Kim, H., Han, M., Kim, T., 2019. Generation of sub-micron (nano) bubbles and characterization of their fundamental properties. Environmental Engineering Research 24, 382–388. https://doi.org/10.4491/eer.2018.210.
H, Klammler, Mohamed Mohamed, M.A., Kirk, Hatfield, Jerry, A., Jung, J., 2020. Modeling micro- and nano-bubble stability and treatment mechanisms in batch reactors. J. Environ. Eng. 146, 04020079 https://doi.org/10.1061/(ASCE)EE.1943-7870.0001736.
Klemeshev, S.A., Petrov, M.P., Rolich, V.I., Trusov, A.A., Voitylov, A.V., Vojtylov, V.V., 2016. Static, dynamic and electric light scattering by aqueous colloids of diamond. Diam. Relat. Mater. 69, 177–182. https://doi.org/10.1016/j.diamond.2016.08.016.
Komaba, K., Goto, H., 2019. Micro-bubble sonic-electrochemical preparation of polyaniline. ECS Trans 92, 57. https://doi.org/10.1149/09210.0057ecst.
Koshoridze, S.I., Levin, Y.K., 2019. Thermodynamic analysis OF the stability OF nanobubbles IN water. NST 10. https://doi.org/10.1615/NanoSciTechnolIntJ.2018028801.
Kwon, H., Mohamed, M.M., Annable, M.D., Kim, H., 2020. Remediation of NAPL-contaminated porous media using micro-nano ozone bubbles: bench-scale experiments. J. Contam. Hydrol. 228, 103563.
Li, P., Takahashi, M., Chiba, K., 2009. Enhanced free-radical generation by shrinking microbubbles using a copper catalyst. Chemosphere 77, 1157–1160.
Li, H., Hu, L., Song, D., Al-Tabbaa, A., 2013a. Subsurface transport behavior of micro-nano bubbles and potential applications for groundwater remediation. Int. J. Environ. Res. Publ. Health 11, 473–486. https://doi.org/10.3390/ijerph110100473.
Li, H., Hu, L., Xia, Z., 2013b. Impact of groundwater salinity on bioremediation enhanced by micro-nano bubbles. Materials 6, 3676–3687. https://doi.org/10.3390/ma6093676.
Li, H., Hu, L., Song, D., Lin, F., 2014. Characteristics of micro-nano bubbles and potential application in groundwater bioremediation. Water Environ. Res. 86, 844–851. https://doi.org/10.2175/106143014X14062131177953.
Li, H., Hu, L., Xin, H., 2015. Application of micro-nano bubble technology in remediation of polluted groundwater. Chin. J. Geotech. Eng. 37, 115–120.
Li, C., Zhang, A.-M., Wang, S., Cui, P., 2018. Formation and coalescence of nanobubbles under controlled gas concentration and species. AIP Adv. 8, 015104 https://doi.org/10.1063/1.5013244.
Li, M., Bussonnière, A., Bronson, M., Xu, Z., Liu, Q., 2019a. Study of Venturi tube geometry on the hydrodynamic cavitation for the generation of microbubbles. Miner. Eng. 132, 268–274. https://doi.org/10.1016/j.mineng.2018.11.001.
Li, Y., Yang, G., Yu, S., Kang, Z., Mo, J., Han, B., Talley, D.A., Zhang, F.-Y., 2019b. In-situ investigation and modeling of electrochemical reactions with simultaneous oxygen and hydrogen microbubble evolutions in water electrolysis. Int. J. Hydrogen Energy 44, 28283–28293. https://doi.org/10.1016/j.ijhydene.2019.09.044.
Li, P., Ma, Y., Zhu David, Z., 2020. Mass transfer of gas bubbles rising in stagnant water. J. Environ. Eng. 146, 04020084 https://doi.org/10.1061/(ASCE)EE.1943-7870.0001760.
Liu, C., Tang, Y., 2019. Application research of micro and nano bubbles in water pollution control. E3S Web Conf 136, 06028. https://doi.org/10.1051/e3sconf/201913606028.
Liu, S., Wang, Q., Sun, T., Wu, C., Shi, Y., 2012. The effect of different types of micro-bubbles on the performance of the coagulation flotation process for coke waste-water. J. Chem. Technol. Biotechnol. 87, 206–215. https://doi.org/10.1002/jctb.2698.
Liu, Y., Ke, H., Ba, T., Wu, X.W., 2018. Study on the cleaning of organic pollutants by micronano bubbles in sandy soil foundation. In: The International Congress on Environmental Geotechnics. Springer, pp. 859–867.
Lucero, A., Kim, D.-S., Park, Y.-S., 2017. Parameter optimization for cost reduction of microbubble generation by electrolysis. J. Environ. Sci. 26, 269–280.
Ma, Y., Kong, X.Z., Scheuermann, A., Galindo-Torres, S.A., Bringemeier, D., Li, L., 2015. Microbubble transport in water-saturated porous media. Water Resour. Res. 51, 4359–4373. https://doi.org/10.1002/2014WR016019.
Ma, T., Kimura, Y., Yamamoto, H., Feng, X., Hirano-Iwata, A., Niwano, M., 2020. Characterization of bulk nanobubbles formed by using a porous alumina film with ordered nanopores. J. Phys. Chem. B. https://doi.org/10.1021/acs.jpcb.0c02279.
Majid, A.I., Nugroho, F.M., Juwana, W.E., Budhijanto, W., Deendarlianto, Indarto, 2018. On the performance of venturi-porous pipe microbubble generator with inlet angle of 20° and outlet angle of 12°. In: AIP Conference Proceedings 2001, 050009 https://doi.org/10.1063/1.5050000.
Maxwell, J., 2020. Oxygen Generation Device, US20200047109A1.
Meegoda, J.N., Aluthgun Hewage, S., Batagoda, J.H., 2018. Stability of nanobubbles. Environ. Eng. Sci. 35, 1216–1227. https://doi.org/10.1089/ees.2018.0203.
Melich, R., Valour, J.-P., Urbaniak, S., Padilla, F., Charcosset, C., 2019. Preparation and characterization of perfluorocarbon microbubbles using Shirasu Porous Glass (SPG) membranes. Colloid. Surf. A: Physicochem. Eng. Aspect. 560, 233–243. https://doi.org/10.1016/j.colsurfa.2018.09.058.
Midtvedt, D., Eklund, F., Olsén, E., Midtvedt, B., Swenson, J., Höök, F., 2020. Size and refractive index determination of subwavelength particles and air bubbles by holographic nanoparticle tracking analysis. Anal. Chem. 92, 1908–1915. https://doi.org/10.1021/acs.analchem.9b04101.
Miller, R.R., 1996. Bioslurping: Technology Overview Report.
Moruzzi, R.B., Reali, M. a. P., 2010. Characterization of micro-bubble size distribution and flow configuration in DAF contact zone by a non-intrusive image analysis system and tracer tests. Water Sci. Technol. 61, 253–262. https://doi.org/10.2166/wst.2010.784.
Morito, H., Makuta, T., 2018. Development and optimization of a microbubble generator with a hollow cylindrical ultrasonic horn. J. Chem. Eng. Jpn. 51, 175–179.
Moyo, P., Gomez, C.O., Finch, J.a., 2007. Characterizing frothers using water carrying rate. Canadian Metallurgical Quarterly 46, 215–220. https://doi.org/10.1179/000844307794566007.
Nam, G., Mohamed, M.M., Jung, J., 2019. Enhanced degradation of benzo[a]pyrene and toxicity reduction by microbubble ozonation. Environ. Technol. 1–8. https://doi.org/10.1080/09593330.2019.1683077.
Nirmalkar, N., Pacek, A.W., Barigou, M., 2018a. On the existence and stability of bulk nanobubbles. Langmuir 34, 10964–10973. https://doi.org/10.1021/acs.langmuir.8b01163.
Nirmalkar, N.W., Pacek, A., Barigou, M., 2018b. Interpreting the interfacial and colloidal stability of bulk nanobubbles. Soft Matter 14, 9643–9656. https://doi.org/10.1039/C8SM01949E.
Nock, W.J., 2015. An Investigation into Gas Transfer from Bubbles into Water (phd). University of Southampton.
Numakura, T., Kashiwagura, K., Makuta, T., 2014. Development and optimization of a microbubble generator with a hollow cylindrical ultrasonic horn. Journal of the Japanese Society for Experimental Mechanics 14, s52–s56.
Oliveira, H.A., Azevedo, A.C., Etchepare, R., Rubio, J., 2017. Separation of emulsified crude oil in saline water by flotation with micro- and nanobubbles generated by a multiphase pump. Water Sci. Technol. 76, 2710–2718. https://doi.org/10.2166/wst.2017.441.
Pambudiarto, B.A., Mindaryani, A., Deendarlianto, D., Budhijanto, W., 2020. Evaluation of the effect of operating parameters on the performance of orifice/porous pipe type micro-bubble generator. Journal of Engineering and Technological Sciences 52, 196–207. https://doi.org/10.5614/j.eng.technol.sci.2020.52.2.5, 207.
Park, J.Y., Choi, Y.J., Moon, S., Shin, D.Y., Nam, K., 2009. Microbubble suspension as a carrier of oxygen and acclimated bacteria for phenanthrene biodegradation. J. Hazard Mater. 163, 761–767. https://doi.org/10.1016/j.jhazmat.2008.07.024.
Park, Y., Diez-Silva, M., Fu, D., Popescu, G., Choi, W., Barman, I., Suresh, S., Feld, M.S., 2010. Static and dynamic light scattering of healthy and malaria-parasite invaded red blood cells. J. Biomed. Optic. 15, 020506.
Parkinson, L., Sedev, R., Fornasiero, D., Ralston, J., 2008. The terminal rise velocity of 10–100 μm diameter bubbles in water. J. Colloid Interface Sci. 322, 168–172. https://doi.org/10.1016/j.jcis.2008.02.072.

Parmar, R., Majumder, S.K., 2013. Microbubble generation and microbubble-aided transport process intensification-A state-of-the-art report. Chem. Eng. Process: Process Intensification 64, 79–97. https://doi.org/10.1016/j.cep.2012.12.002.

Parmar, R., Majumder, S.K., 2015. Terminal rise velocity, size distribution and stability of microbubble suspension. Asia Pac. J. Chem. Eng. 10, 450–465. https://doi.org/10.1002/apj.1891.

Pérez-Garibay, R., Martínez-Ramos, E., Rubio, J., 2012. Gas dispersion measurements in microbubble flotation systems. Miner. Eng. 26, 34–40. https://doi.org/10.1016/j.mineng.2011.10.006.

Pérez-Lucas, G., Vela, N., El Aatik, A., Navarro, S., 2019. Environmental risk of groundwater pollution by pesticide leaching through the soil profile. In: Larramendy, M., Soloneski, S. (Eds.), Pesticides - Use and Misuse and Their Impact in the Environment. IntechOpen. https://doi.org/10.5772/intechopen.82418.

Postnikov, A.V., Uvarov, I.V., Lokhanin, M.V., Svetovoy, V.B., 2016. Highly energetic phenomena in water electrolysis. Sci. Rep. 6, 39381.

Postnikov, A.V., Uvarov, I.V., Penkov, N.V., Svetovoy, V.B., 2018. Collective behavior of bulk nanobubbles produced by alternating polarity electrolysis. Nanoscale 10, 428–435.

Qian, J., Craig, V.S.J., Jehannin, M., 2019. Long-term stability of surface nanobubbles in undersaturated aqueous solution. Langmuir 35, 718–728. https://doi.org/10.1021/acs.langmuir.8b03487.

Rajah, Z., Guiza, M., Solís, R.R., Rivas, F.J., Ouederni, A., 2019. Catalytic and photocatalytic ozonation with activated carbon as technologies in the removal of aqueous micropollutants. J. Photochem. Photobiol. Chem. 382, 111961. https://doi.org/10.1016/j.jphotochem.2019.111961.

Ren, L., Zhang, Y., Qin, W., Bao, S., Wang, P., Yang, C., 2014. Investigation of condition-induced bubble size and distribution in electroflotation using a high-speed camera. Int. J. Min. Sci. Technol. 24, 7–12. https://doi.org/10.1016/j.ijmst.2013.12.002.

Rizaldi, M.I., Rahman, A., Deendarlianto, Prihantini, N.B., Nasruddin, 2019. Generation of microbubbles through single loop and double loop fluid oscillator for photobioreactor aeration. International Journal of Technology 10, 1446–1452. https://doi.org/10.14716/ijtech.v10i7.3691.

Rosa, A.F., Rubio, J., 2018. On the role of nanobubbles in particle–bubble adhesion for the flotation of quartz and apatitic minerals. Miner. Eng. 127, 178–184. https://doi.org/10.1016/j.mineng.2018.08.020.

Ryskie, S., Gonzalez-Merchan, C., Neculita, C.M., Genty, T., 2020. Efficiency of ozone microbubbles for ammonia removal from mine effluents. Miner. Eng. 145, 106071. https://doi.org/10.1016/j.mineng.2019.106071.

Sadatomi, M., Kawahara, A., Kano, K., Ohtomo, A., 2005. Performance of a new micro-bubble generator with a spherical body in a flowing water tube. Exp. Therm. Fluid Sci. 29, 615–623. https://doi.org/10.1016/j.expthermflusci.2004.08.006.

Sadatomi, M., Kawahara, A., Matsuura, H., Shikatani, S., 2012. Micro-bubble generation rate and bubble dissolution rate into water by a simple multi-fluid mixer with orifice and porous tube. Exp. Therm. Fluid Sci. 41, 23–30. https://doi.org/10.1016/j.expthermflusci.2012.03.002.

Saijai, S., Thonglek, V., Yoshikawa, K., 2019. Sterilization effects of ozone fine (micro/nano) bubble water. International Plasma Environmental Science and Technology 12, 55–58.

Shafi, A.S., McClements, J., Albaijan, I., Abou-Saleh, R.H., Moran, C., Koutsos, V., 2019. Probing phospholipid microbubbles by atomic force microscopy to quantify bubble mechanics and nanostructural shell properties. Colloids Surf. B Biointerfaces 181, 506–515. https://doi.org/10.1016/j.colsurfb.2019.04.062.

Shams, M., Dehghani, M.H., Nabizadeh, R., Mesdaghinia, A., Alimohammadi, M., Najafpoor, A.A., 2016. Adsorption of phosphorus from aqueous solution by cubic zeolitic imidazolate framework-8: modeling, mechanical agitation versus sonication. J. Mol. Liq. 224, 151–157. https://doi.org/10.1016/j.molliq.2016.09.059.

Shangguan, Y., Yu, S., Gong, C., Wang, Y., Yang, W., Hou, L., 2018. A review of microbubble and its applications in ozonation. IOP Conf. Ser. Earth Environ. Sci. 128, 012149 https://doi.org/10.1088/1755-1315/128/1/012149.

Shi, W., Pan, G., Chen, Q., Song, L., Zhu, L., Ji, X., 2018. Hypoxia remediation and methane emission manipulation using surface oxygen nanobubbles. Environ. Sci. Technol. 52, 8712–8717. https://doi.org/10.1021/acs.est.8b02320.

Skouteris, G., Rodriguez-Garcia, G., Reinecke, S.F., Hampel, U., 2020. The use of pure oxygen for aeration in aerobic wastewater treatment: a review of its potential and limitations. Bioresour. Technol. 312, 123595. https://doi.org/10.1016/j.biortech.2020.123595.

Smith, B., 2015. The Differences between Atomic Force Microscopy and Scanning Electron Microscopy [WWW Document]. AZoM.com, 6.17.20. https://www.azom.com/article.aspx?ArticleID=11879.

Song, D., Katayama, A., 2010. Approach for estimating microbial growth and the biodegradation of hydrocarbon contaminants in subsoil based on field measurements: 1. Model development and verification. Environ. Sci. Technol. 44, 767–773. https://doi.org/10.1021/es9017199.

On the effect of the internal friction of fluids on the motion of pendulums. In: Stokes, G. G. (Ed.), 2009. Mathematical and Physical Papers, Cambridge Library Collection - Mathematics. Cambridge University Press, Cambridge, pp. 1–10. https://doi.org/10.1017/CBO9780511702266.002.

Stride, E., Edirisinghe, M., 2009. Novel preparation techniques for controlling microbubble uniformity: a comparison. Med. Biol. Eng. Comput. 47, 883–892. https://doi.org/10.1007/s11517-009-0490-8.

Sun, Y., Xie, G., Peng, Y., Xia, W., Sha, J., 2016. Stability theories of nanobubbles at solid–liquid interface: a review. Colloid. Surface. Physicochem. Eng. Aspect. 495, 176–186. https://doi.org/10.1016/j.colsurfa.2016.01.050.

Sun, H., Liu, H., Wang, S., Liu, Y., 2019. Remediation of oil spill-contaminated sands by chemical-free microbubbles generated in tap and saline water. J. Hazard Mater. 366, 124–129. https://doi.org/10.1016/j.jhazmat.2018.11.102.

Sun, Z., Xia, F., Lou, Z., Chen, X., Zhu, N., Yuan, H., Shen, Y., 2020. Innovative process for total petroleum hydrocarbons reduction on oil refinery sludge through microbubble ozonation. J. Clean. Prod. 256, 120337. https://doi.org/10.1016/j.jclepro.2020.120337.

Suwartha, N., Syamzida, D., Priadi, C.R., Moersidik, S.S., Ali, F., 2020. Effect of size variation on microbubble mass transfer coefficient in flotation and aeration processes. Heliyon 6, e03748. https://doi.org/10.1016/j.heliyon.2020.e03748.

Svetovoy, V.B., Sanders, R.G.P., Lammerink, T.S.J., Elwenspoek, M.C., 2011. Combustion of hydrogen-oxygen mixture in electrochemically generated nanobubbles. Phys. Rev. E 84, 035302. https://doi.org/10.1103/PhysRevE.84.035302.

Svetovoy, V.B., Sanders, R.G.P., Elwenspoek, M.C., 2013. Transient nanobubbles in short-time electrolysis. J. Phys. Condens. Matter 25, 184002. https://doi.org/10.1088/0953-8984/25/18/184002.

Svetovoy, V.B., Prokaznikov, A.V., Postnikov, A.V., Uvarov, I.V., Palasantzas, G., 2020. Explosion of microbubbles generated by the alternating polarity water electrolysis. Energies 13, 20. https://doi.org/10.3390/en13010020.

Swart, B., Zhao, Y., Khaku, M., Che, E., Maltby, R., Chew, Y.M.J., Wenk, J., 2020. In situ characterisation of size distribution and rise velocity of microbubbles by high-speed photography. Chem. Eng. Sci. 225, 115836. https://doi.org/10.1016/j.ces.2020.115836.

Takahashi, M., 2005. ζ potential of microbubbles in aqueous solutions: electrical properties of the Gas−Water interface. J. Phys. Chem. B 109, 21858–21864. https://doi.org/10.1021/jp0445270.

Takahashi, M., Chiba, K., Li, P., 2007a. Free-radical generation from collapsing microbubbles in the absence of a dynamic stimulus. J. Phys. Chem. B 111, 1343–1347. https://doi.org/10.1021/jp0669254.

Takahashi, M., Chiba, K., Li, P., 2007b. formation of hydroxyl radicals by collapsing ozone microbubbles under strongly acidic conditions. J. Phys. Chem. B 111, 11443–11446. https://doi.org/10.1021/jp074727m.

Takahashi, M., Ishikawa, H., Asano, T., Horibe, H., 2012. Effect of microbubbles on ozonized water for photoresist removal. J. Phys. Chem. C 116, 12578–12583. https://doi.org/10.1021/jp301746g.

Talabi, A.O., Kayode, T.J., 2019. Groundwater pollution and remediation. JWARP 11, 1–19. https://doi.org/10.4236/jwarp.2019.111001.

Tanaka, S., Kastens, S., Fujioka, S., Schlüter, M., Terasaka, K., 2020. Mass transfer from freely rising microbubbles in aqueous solutions of surfactant or salt. Chem. Eng. J. 387, 121246. https://doi.org/10.1016/j.cej.2019.03.122.

Tao, W., 2018. Transport of Bacteria in Column for in Situ Bioremediation Application: Effect of Dissolved Surfactant and Microbubble on Bacterial Mobility in Sand (Thesis). ResearchSpace@Auckland.

Tekile, A., Kim, I., Lee, J.-Y., 2017. Applications of ozone micro-and nanobubble technologies in water and wastewater treatment. 상하수도학회지 31, 481–490.

Temesgen, T., Bui, T.T., Han, M., Kim, T. il, Park, H., 2017. Micro and nanobubble technologies as a new horizon for water-treatment techniques: a review. Adv. Colloid Interface Sci. 246, 40–51. https://doi.org/10.1016/j.cis.2017.06.011.

Thonglek, V., Yoshikawa, K., Tokuda, Y., Ueda, Y., 2019. Identification of high concentration ultra-fine bubbles in the water. IJPEST 12, 89–92.

Turner, W.R., 1961. Microbubble Persistence in Fresh Water. J. Acoust. Soc. Am. 33, 1223–1233. https://doi.org/10.1121/1.1908960.

Ulatowski, K., Sobieszuk, P., Mróz, A., Ciach, T., 2019. Stability of nanobubbles generated in water using porous membrane system. Chemical Engineering and Processing - Process Intensification 136, 62–71. https://doi.org/10.1016/j.cep.2018.12.010.

Ushikubo, F.Y., Enari, M., Furukawa, T., Nakagawa, R., Makino, Y., Kawagoe, Y., Oshita, S., 2010a. Zeta-potential of micro- and/or nano-bubbles in water produced by some kinds of gases. In: IFAC Proceedings Volumes, 3rd IFAC Conference in Modelling and Control in Agriculture, Horticulture and Post-Harvest Processing - Agricontrol, vol. 43, pp. 283–288. https://doi.org/10.3182/20101206-3-JP-3009.00050.

Ushikubo, F.Y., Furukawa, T., Nakagawa, R., Enari, M., Makino, Y., Kawagoe, Y., Shiina, T., Oshita, S., 2010b. Evidence of the existence and the stability of nano-bubbles in water. Colloid. Surface. Physicochem. Eng. Aspect. 361, 31–37. https://doi.org/10.1016/j.colsurfa.2010.03.005.

Vakarelski, I.U., Manica, R., Tang, X., O'Shea, S.J., Stevens, G.W., Grieser, F., Dagastine, R.R., Chan, D.Y.C., 2010. Dynamic interactions between microbubbles in water. Proc. Natl. Acad. Sci. U. S. A. 107, 11177–11182. https://doi.org/10.1073/pnas.1005937107.

Vion, P., 2007. Pressurised Water Pressure-Reducing Nozzle for Generating Microbubbles in a Flotation Plant, US20070119987A1.

Wang, H., Zhang, L., 2017. Research on the nitrogen removal efficiency and mechanism of deep subsurface wastewater infiltration systems by fine bubble aeration. Ecol. Eng. 107, 33–40. https://doi.org/10.1016/j.ecoleng.2017.07.005.

Wang, Y., Fan, J.-N., Yang, Y., Zhang, Y., Cao, Z., Wang, T., 2019. Statistical analysis of jet drop generation based on bubble size measurements in the pickling process. Build. Environ. 155, 25–33. https://doi.org/10.1016/j.buildenv.2019.03.044.

Wang, L., Miao, X., Ali, J., Lyu, T., Pan, G., 2018. Quantification of oxygen nanobubbles in particulate matters and potential applications in remediation of anaerobic environment. ACS Omega 3, 10624–10630. https://doi.org/10.1021/acsomega.8b00784.

Wei Lu, G., Ping, G., 2010. Handbook of Non-invasive Drug Delivery Systems-Chapter 3 Emulsions and Microemulsions for Topical and Transdermal Drug Delivery.

Weiner, B.B., Zhang, Y., 2013. How to choose a zeta potential analyzer: general guidelines [WWW Document]. https://www.brookhaveninstruments.com/wp-content/uploads/2019/11/guide-to-choosing-zeta-potential-analyzer-brookhaven-instruments.pdf.

Xia, Z., Hu, L., 2019a. Theoretical model for micro-nano-bubbles mass transfer during contaminant treatment. J. Environ. Eng. Sci. 14, 157–167. https://doi.org/10.1680/jenes.18.00039.
Xia, Z., Hu, L., 2019b. Treatment of organics contaminated wastewater by ozone micro-nano-bubbles. Water 11, 55. https://doi.org/10.3390/w11010055.
Xia, Z., Hu, L., Kusaba, S., Song, D., 2019. Remediation of TCE contaminated site by ozone micro-nano-bubbles. In: Zhan, L., Chen, Y., Bouazza, A. (Eds.), Proceedings of the 8th International Congress on Environmental Geotechnics Volume 1, Environmental Science and Engineering. Springer, Singapore, pp. 796–803. https://doi.org/10.1007/978-981-13-2221-1_90.
Xiao, W., Xu, G., 2020. Mass transfer of nanobubble aeration and its effect on biofilm growth: microbial activity and structural properties. Sci. Total Environ. 703, 134976. https://doi.org/10.1016/j.scitotenv.2019.134976.
Xiao, W., Ke, S., Quan, N., Zhou, L., Wang, J., Zhang, L., Dong, Y., Qin, W., Qiu, G., Hu, J., 2018. The role of nanobubbles in the precipitation and recovery of organic-phosphine-containing beneficiation wastewater. Langmuir 34, 6217–6224. https://doi.org/10.1021/acs.langmuir.8b01123.
Xiong, Y., Yang, X., Song, Hailiang, 2016. Review ON application OF micro-nano bubble IN water treatment and its generator. Water Pollut. Control 6, 23–27. https://doi.org/10.13205/j.hjgc.201606006.
Xiong, X., Wang, B., Zhu, W., Tian, K., Zhang, H., 2019. A review on ultrasonic catalytic microbubbles ozonation processes: properties, hydroxyl radicals generation pathway and potential in application. Catalysts 9, 10. https://doi.org/10.3390/catal9010010.
Xu, R., 2008. Progress in nanoparticles characterization: sizing and zeta potential measurement. Particuology 6, 112–115. https://doi.org/10.1016/j.partic.2007.12.002.
Xu, Q., Nakajima, M., Ichikawa, S., Nakamura, N., Shiina, T., 2008. A comparative study of microbubble generation by mechanical agitation and sonication. Innovat. Food Sci. Emerg. Technol. 9, 489–494. https://doi.org/10.1016/j.ifset.2008.03.003.
Yamaguchi, T., Ishikawa, T., Imai, Y., 2018. Integrated Nano-Biomechanics- Chapter 4 Biomechanics for Pathology and Treatment.
Yasuda, K., Matsushima, H., Asakura, Y., 2019. Generation and reduction of bulk nanobubbles by ultrasonic irradiation. Chem. Eng. Sci. 195, 455–461. https://doi.org/10.1016/j.ces.2018.09.044.
Yasui, K., Tuziuti, T., Kanematsu, W., 2018. Mysteries of bulk nanobubbles (ultrafine bubbles); stability and radical formation. Ultrason. Sonochem. 48, 259–266. https://doi.org/10.1016/j.ultsonch.2018.05.038.
Yoshida, A., Takahashi, O., Ishii, Y., Sekimoto, Y., Kurata, Y., 2008. Water purification using the adsorption characteristics of microbubbles. Jpn. J. Appl. Phys. 47, 6574–6577. https://doi.org/10.1143/JJAP.47.6574.
Yujing, W., 2018. Advances and challenges in oxidation of micro-nano bubbles for water decontamination. Chemical Engineering Design Communications 44, 216–217. https://doi.org/10.3969/j.issn.1003-6490.2018.09.187.
Zhang, W., 2016. The effects of frothers and particles on the characteristics of pulp and froth properties in flotation—a critical review. J. Miner. Mater. Char. Eng. 4, 251–269. https://doi.org/10.4236/jmmce.2016.44023.
Zhang, M., Cai, Z., Xie, L., Zhang, Y., Tang, L., Zhou, Q., Qiang, Z., Zhang, H., Zhang, D., Pan, X., 2019. Comparison of coagulative colloidal microbubbles with monomeric and polymeric inorganic coagulants for tertiary treatment of distillery wastewater. Sci. Total Environ. 694, 133649. https://doi.org/10.1016/j.scitotenv.2019.133649.
Zhang, H., Chen, J., Han, M., An, W., Yu, J., 2020a. Anoxia remediation and internal loading modulation in eutrophic lakes using geoengineering method based on oxygen nanobubbles. Sci. Total Environ. 714, 136766. https://doi.org/10.1016/j.scitotenv.2020.136766.
Zhang, X., Wang, Q., Wu, Z., Tao, D., 2020b. An experimental study on size distribution and zeta potential of bulk cavitation nanobubbles. ijmmm 27, 152–161. https://doi.org/10.1007/s12613-019-1936-0.
Zhang, M., Yang, J., Tang, L., Zhang, D., Pan, X., 2020. Lability-specific enrichment of typical engineered metal (oxide) nanoparticles by surface-functionalized microbubbles from waters. Sci. Tot. Environ. 719, 137526. https://doi.org/10.1016/j.scitotenv.2020.137526.
Zhao, S., Yao, C., Dong, Z., Liu, Y., Chen, G., Yuan, Q., 2018. Intensification of liquid-liquid two-phase mass transfer by oscillating bubbles in ultrasonic microreactor. Chem. Eng. Sci. 186, 122–134. https://doi.org/10.1016/j.ces.2018.04.042.
Zheng, T., Wang, Q., Zhang, T., Shi, Z., Tian, Y., Shi, S., Smale, N., Wang, J., 2015. Microbubble enhanced ozonation process for advanced treatment of wastewater produced in acrylic fiber manufacturing industry. J. Hazard Mater. 287, 412–420. https://doi.org/10.1016/j.jhazmat.2015.01.069.
Zhou, S., Wang, X., Bu, X., Wang, M., An, B., Shao, H., Ni, C., Peng, Y., Xie, G., 2020. A novel flotation technique combining carrier flotation and cavitation bubbles to enhance separation efficiency of ultra-fine particles. Ultrason. Sonochem. 64, 105005. https://doi.org/10.1016/j.ultsonch.2020.105005.
Zimmerman, W.B., Tesar, V., Bandulasena, S.B. and H.C.H., 2007. Microbubble Generation [WWW Document]. Recent Patents on Engineering. URL https://www.eurekaselect.com/92515/article (accessed 6.28.20).